

A Unified View of Allostery.

Eric Rouviere

*Center for Physics of Evolving Systems, Department of Biochemistry & Molecular Biology,
University of Chicago, Chicago, IL, USA, 60637 and
Graduate Program in Biophysical Sciences, University of Chicago, Chicago, IL, USA, 60637*

Olivier Rivoire

Gulliver, ESPCI Paris, CNRS, Université PSL, 75005 Paris, France

Rama Ranganathan

*Center for Physics of Evolving Systems, Department of Biochemistry & Molecular Biology,
University of Chicago, Chicago, IL, USA, 60637 and
The Pritzker School for Molecular Engineering, University of Chicago, Chicago, IL, USA, 60637*

Allostery is a fundamental property of proteins that represents the functional coupling between distantly located sites. In different manifestations, this property underlies signal transduction, gene expression, and regulation—elementary reactions in networks comprising cellular information and metabolic processing systems. In this work, we present a reduced theoretical model for allostery that encompasses the many diverse mechanisms described in past work. What emerges is a basic classification of different forms of allostery into two groups: those that couple distant sites through soft normal modes within a single state, and those that possess multiple states, with effective interactions between sites emerging only upon transitioning between these states. This work serves to unify the extensive past theoretical work on the phenomenology and machinery of allostery in proteins.

Keywords: Allostery, Cooperativity, Dynamics, Multiple States

Allostery is a fundamental property of proteins involved in nearly all cellular processes [1–3]. In its essence, it describes the thermodynamic coupling of two sites of a protein when they do not directly interact. This coupling, often termed cooperativity, is a thermodynamic phenomenon and thus its existence is agnostic to the physical mechanism through which it is implemented.

Various theoretical models have been proposed to explain allostery, each differing in their level of physical detail. At the most abstract level, thermodynamic (or phenomenological) models reduce the high-dimensional conformational space that proteins sample into a few discrete states and define rules for the free energy of each state [4–10]. While these models have successfully explained and fit data [4–6, 11, 12], they lack the detail needed to describe the physics of allosteric mechanisms.

On the other hand, molecular dynamics models define the chemical interactions between all atoms, enabling granular descriptions of the sequence of motions in allosteric transitions [13–15]. However, this level of detail makes it challenging to separate general principles from features unique to individual proteins.

Between these two extremes live reduced physical models that assume simplified interactions between coarse-grained amino acid groups. A common example is elastic network models, where amino acid groups interact through ideal springs, and structural motions are approximated within linear response [16–18]. These simplifications allow for exact computation of allosteric cooperativity between binding sites [19–21]. However, a drawback of these models is that they often rely on assump-

tions that limit the range of possible allosteric behaviors. For instance, the linear response approximation in elastic networks prevents the existence of multiple metastable conformational states.

The wide variety of models has led to numerous proposed forms of allostery, each emphasizing different key physical behaviors, such as multiple conformational states [4, 22–25], changes in protein dynamics upon binding [19, 26, 27], and folding and intrinsic disorder [9]. What remains unclear is how these different models of allostery relate to one another. Are they simply alternative implementations of the same underlying principle, or do they rely on fundamentally distinct principles? If the latter, how many unique principles can enable allostery?

To address these questions we present a physical framework in which a protein has two non-overlapping binding sites and investigate the conditions in which ligand binding is allosterically coupled. We assume a generic form of an energy landscape that can approximate any protein, and show that only two physical principles can enable allostery. The first principle is to have soft normal modes (low energy correlated motions around a structure) couple the two sites with ligand binding engaging the same modes from both sites. This is the only solution when a protein’s energy landscape is described by a single energy basin. The second principle requires two or more states that bind ligands with different affinities—the same principle described by the well-known MWC model [4]. We show, that different physical implementations of each principle correspond to previously proposed forms of allostery.

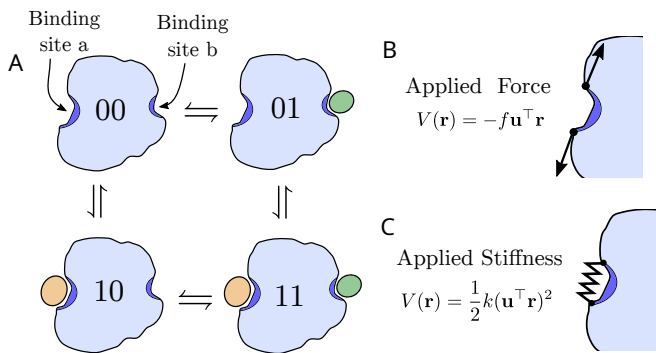


FIGURE 1. Formulation of the model. (A) The model considers a protein with two binding sites, (a and b) leading to 4 distinct ligation conditions labeled 00, 10, 01, 11 for apo, bound at a , bound at b , and doubly bound, respectively. Two forms of ligand perturbations along a binding mode \mathbf{u} are considered: (B) an applied constant force that is mathematically represented as a perturbation of the form $-f \mathbf{u}^T \mathbf{r}$. (C) An applied stiffness by adding a spring between two beads at the site that is mathematically represented by $\frac{1}{2} k (\mathbf{u}^T \mathbf{r})^2$.

Previous works have unified allosteric models at the thermodynamic level [6, 7, 10, 28], however, this level of description lacks the notion of normal modes. Consequently, the soft mode principle is missed and forms of allostery that depend on this principle [19–21, 26, 27, 29–32] are not described by these unifications. By considering genetic energy landscapes we overcome this limitation and make inroads toward a general physical theory of allostery.

RESULTS

The model

The model comprises a “system” made up of N parts (e.g. amino acids) with no constraint placed on the details of the internal structure. Thus, the system is simply represented as shapes in Figure 1A. But, the parts comprising the system are specified to interact through a global potential $U_p(\mathbf{r})$ that is a function of the positions of the parts $\mathbf{r} = (\mathbf{r}_1, \mathbf{r}_2, \dots, \mathbf{r}_N)$, where $\mathbf{r}_i = (x_i, y_i, z_i)$. This construction allows us to consider various forms of $U_p(\mathbf{r})$ that in the sections below, will clarify the most fundamental physical principle underlying allostery.

To implement the idea of allostery, we define two distantly positioned binding sites (designated as a and b and marked by orange and green ligands, Figure 1A). Ligand binding to these sites is modeled as a change to the energy landscape and is represented mathematically through perturbations $V_a(\mathbf{r}), V_b(\mathbf{r})$. There are four ligation states of the system—unbound, bound at either site, or bound at both. With indicator variables σ_a, σ_b that take value 1 if the ligand is bound to the site and 0 if unbound, we can write the energy landscapes of the four

binding conditions (unbound: $\sigma_a = \sigma_b = 0$, bound at a : $\sigma_a = 1, \sigma_b = 0$, bound at b : $\sigma_a = 0, \sigma_b = 1$ and doubly bound: $\sigma_a = \sigma_b = 1$) as

$$U_{\sigma_a \sigma_b}(\mathbf{r}) = U_p(\mathbf{r}) + \sigma_a V_a(\mathbf{r}) + \sigma_b V_b(\mathbf{r}). \quad (1)$$

The partition function for each energy is $Z_{\sigma_a \sigma_b} = h_0^{-3N} \int d\mathbf{r} \exp(-\beta U_{\sigma_a \sigma_b})$ and the corresponding free energy is $F_{\sigma_a \sigma_b} = -\beta^{-1} \log Z_{\sigma_a \sigma_b}$. We choose units where $h_0 = 1$ and it is omitted going forward.

An allosteric interaction implies that binding at one site alters the binding free energy at the other site. This feature, known as binding cooperativity, is defined as,

$$\Delta \Delta F = (F_{10} - F_{00}) - (F_{11} - F_{01}) = -\frac{1}{\beta} \log \left[\frac{Z_{10} Z_{01}}{Z_{00} Z_{11}} \right]. \quad (2)$$

Positive cooperativity corresponds to the case when $\Delta \Delta F > 0$ and negative cooperativity when $\Delta \Delta F < 0$. Since the free energy is the sum of entropic and entropic contributions $F = E - TS$, the cooperativity also decomposes similarly: $\Delta \Delta F = \Delta \Delta E - T \Delta \Delta S$.

This formulation allows us to connect physical features at the level of the energy landscapes (U_p, V_a, V_b) to allostery at the thermodynamic level, $\Delta \Delta F$. In what follows we first show cooperativity can only occur when the energy landscape U_p satisfies one of two principles: When an energy basin has soft normal modes that couple the two sites or when there are multiple distinguishable states. Then we show how previous models of allostery are specific implementations of these two principles.

Two physical principles enable allostery

For analytical simplicity, we consider ligand potentials that act on a single collective variable that describes a conformational motion of each binding site $\mathbf{u}_a, \mathbf{u}_b$, giving,

$$V_a(\mathbf{r}_a) = g_a(\mathbf{u}_a^T \mathbf{r}), \quad V_b(\mathbf{r}_b) = g_b(\mathbf{u}_b^T \mathbf{r}). \quad (3)$$

The results of this calculation hold for the more general case of arbitrary V_a, V_b (SI). The partition functions can now be expressed as,

$$Z_{\sigma_a \sigma_b} = \int dx_a e^{-\sigma_a \beta g_a(x_a)} \int dx_b e^{-\sigma_b \beta g_b(x_b)} \tilde{Z}(x_a, x_b), \quad (4)$$

$$\tilde{Z}(x_a, x_b) = \int d\mathbf{r} \delta(\mathbf{u}_a^T \mathbf{r} - x_a) \delta(\mathbf{u}_b^T \mathbf{r} - x_b) e^{-\beta U_p(\mathbf{r})}. \quad (5)$$

Taking the log of \tilde{Z} gives a so-called free energy surface of the unperturbed system as a function of the binding site collective variables,

$$\tilde{F}(x_a, x_b) = -\beta^{-1} \log \tilde{Z}(x_a, x_b). \quad (6)$$

If \tilde{F} is separable $\tilde{F}(x_a, x_b) = \tilde{F}_a(x_a) + \tilde{F}_b(x_b)$, both $\tilde{Z}(x_a, x_b)$ and $Z_{\sigma_a \sigma_b}$ factor, leading to no cooperativity

$\Delta\Delta F = 0$. Cooperativity therefore requires \tilde{F} to be non-separable. This implies that the potential for allostery lies in the “protein” landscape U_p even before the physical details of the ligand perturbations are specified.

We assume the energy landscape of a protein may be complex with an arbitrary number of minima. The shape of the energy landscape around each energy minimum \mathbf{R}_i can be approximated by expanding to second order, $U_p(\mathbf{r}) \approx \epsilon_i + \frac{1}{2}(\mathbf{r} - \mathbf{R}_i)^\top H_i(\mathbf{r} - \mathbf{R}_i)$, with $\epsilon_i = U_p(\mathbf{R}_i)$ and $H_i = \nabla\nabla^\top U_p|_{\mathbf{r}=\mathbf{R}_i}$ is the Hessian of U_p at \mathbf{R}_i . By treating each local basin as a state, the full energy landscape can be approximated by summing over the basins,

$$U_p(\mathbf{r}) \approx F_p(\mathbf{r}) = -\frac{1}{\beta} \log \left(\sum_{i=1}^n e^{-\beta \frac{1}{2}(\mathbf{r} - \mathbf{R}_i)^\top H_i(\mathbf{r} - \mathbf{R}_i) + \epsilon_i} \right). \quad (7)$$

This form accurately approximates the regions of an energy landscape that contribute most to the free energy—around the energy minima. The corresponding free energy surface is,

$$\tilde{F}(x_a, x_b) = -\frac{1}{\beta} \log \left(\sum_{i=1}^n C_i e^{-\beta(\frac{1}{2}\mathbf{x}_i^\top A_i^{-1}\mathbf{x}_i + \epsilon_i)} \right), \quad (8)$$

where C_i is a constant for each state i , $\mathbf{x}_i = (x_a - \mathbf{u}_a^\top \mathbf{R}_i, x_b - \mathbf{u}_b^\top \mathbf{R}_i)$ and,

$$A_i = \begin{pmatrix} \mathbf{u}_a^\top H_i^+ \mathbf{u}_a & \mathbf{u}_a^\top H_i^+ \mathbf{u}_b \\ \mathbf{u}_a^\top H_i^+ \mathbf{u}_b & \mathbf{u}_b^\top H_i^+ \mathbf{u}_b \end{pmatrix}. \quad (9)$$

Here H_i^+ is the pseudo-inverse of H_i . Cooperativity can only occur when (8) is not separable, which can occur in two independent ways.

The first way is a property of the curvature of each basin and is most easily seen when only one basin exists, $n = 1$ (for notation we omit the subscripts). In this case, the free energy surface, up to an additive constant, simplifies to $\tilde{F}(x_a, x_b) = \frac{1}{2}\mathbf{x}^\top A^{-1}\mathbf{x}$, and is non-separable only when $|\mathbf{u}_a^\top H^+ \mathbf{u}_b| > 0$. Physically, $\mathbf{u}_a^\top H^+ \mathbf{u}_b$ represents the correlation between the collective variables of the two binding sites. Diagonalizing H^+ expresses this terms in normal modes, $\mathbf{u}_a^\top H^+ \mathbf{u}_b = \mathbf{u}_a^\top Q \Lambda^+ Q^\top \mathbf{u}_b$. The columns of Q are the normal modes of H and thus $Q^\top \mathbf{u}_a$ and $Q^\top \mathbf{u}_b$ describe the overlap of the ligand binding motion with each normal mode. Λ is a diagonal matrix whose entries give the stiffnesses of each normal mode.

When $\mathbf{u}_a^\top H^+ \mathbf{u}_b$ is small, the cooperativity scales as $\Delta\Delta F \sim \mathbf{u}_a^\top H^+ \mathbf{u}_b$ (Methods). This result implies that when a protein’s energy landscape is well described by a single quadratic potential, allostery can only occur when the binding sites are coupled through the normal modes. Furthermore, the contribution of a mode is inversely proportional to its stiffness, making the softest modes the main contributors of cooperativity. We refer to this as the soft mode principle.

The second way cooperativity can occur is when there are multiple, distinct states ($n > 1$). In this case, there are many conditions when \tilde{F} is non-separable even

when the binding sites are uncoupled within each state $\mathbf{u}_a^\top H_i^+ \mathbf{u}_b = 0$. For example, in a two-state landscape, cooperativity is possible when the minima are separated in both x_a and x_b (i.e. $\mathbf{u}_a^\top \mathbf{R}_1 \neq \mathbf{u}_a^\top \mathbf{R}_2$ and $\mathbf{u}_b^\top \mathbf{R}_1 \neq \mathbf{u}_b^\top \mathbf{R}_2$), or when the conformational fluctuations at the binding sites differ in the two states, (i.e. $\mathbf{u}_a H_1^+ \mathbf{u}_a \neq \mathbf{u}_a H_2^+ \mathbf{u}_a$ and $\mathbf{u}_b H_1^+ \mathbf{u}_b \neq \mathbf{u}_b H_2^+ \mathbf{u}_b$).

This case where there exist multiple states and within each state the binding sites are uncoupled ($\mathbf{u}_a^\top H_i^+ \mathbf{u}_b = 0$) corresponds to the key features of the MWC model. We refer to these features as the MWC principle.

This calculation shows that even without describing the physical nature of the ligand perturbations g_a, g_b , one of two physical principles of the protein’s energy landscape must be met for cooperativity to be possible—through soft modes that couple binding sites within a single state (soft mode principle) or by having multiple distinct states (MWC principle). In the following sections, we consider specific cases and show how they encompass previously proposed mechanisms of allostery.

Quadratic Models

What cooperative mechanisms can arise solely from local changes around the minimum of a single basin? To investigate this, we consider the $n = 1$ case of (7) with $\mathbf{R}_1 = \mathbf{0}$ and $\epsilon_1 = 0$ for convenience,

$$U_p = U_{\text{quad}} = \frac{1}{2} \mathbf{r}^\top H \mathbf{r}. \quad (10)$$

For the ligand potentials (3), we consider polynomials up to second order, $g_a(x) = \frac{1}{2}k_a x^2 - f_a x + c_a$ and $g_b(x) = \frac{1}{2}k_b x^2 - f_b x + c_b$. The constant terms do not affect the cooperativity and are set to zero going forward.

When the ligand perturbations have only first-order terms ($k_a = k_b = 0$ giving $V_a(\mathbf{r}) = -f_a \mathbf{u}_a^\top \mathbf{r}$ and $V_b(\mathbf{r}) = -f_b \mathbf{u}_b^\top \mathbf{r}$), which physically correspond to applied forces on the binding sites. The cooperativity computes to (Methods)

$$\Delta\Delta F = f_a f_b \mathbf{u}_a^\top H^+ \mathbf{u}_b. \quad (11)$$

(11) indicates that cooperativity occurs when there are normal modes that couple the binding sites and when the ligand applies forces that push on the same modes in the same direction. Within the context of a particular physical system, structural rigidity imposes constraints on the normal mode structure. In particular, as a folded protein must maintain some stiffness, cooperativity is optimized by making only some modes softer. Negative cooperativity $\Delta\Delta F < 0$ is optimized under the same conditions as positive cooperativity except that ligand forces must push the soft modes in opposite directions. In both cases, the cooperativity is purely energetic with no change in entropy upon ligand binding $\Delta\Delta F = \Delta\Delta E$. This form of cooperativity, previously calculated in different quadratic allosteric models [20, 33–35] follows the induced fit

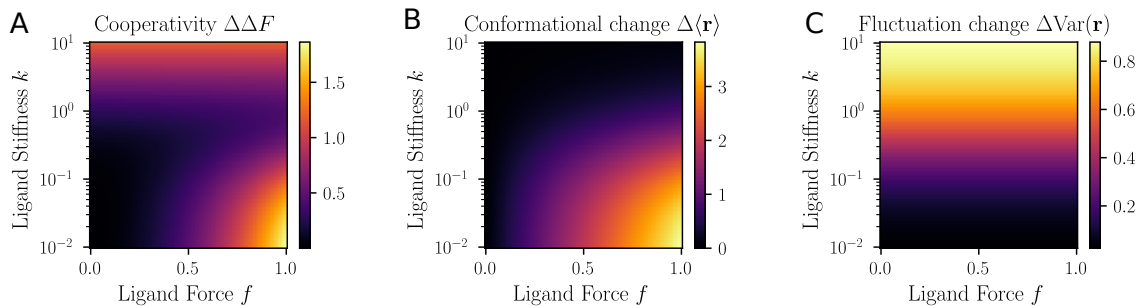


FIGURE 2. Cooperativity with quadratic landscapes. (a) Cooperativity $\Delta\Delta F$, (b) mean conformational change upon ligand binding $\Delta\langle\mathbf{r}\rangle$, and (c) change in the magnitude of fluctuations upon ligand binding $\Delta\text{Var}(\mathbf{r})$, of a quadratic model with a soft mode where ligand binding can apply a force of magnitude f , stiffen with magnitude k or both. The two types of perturbation at each site (force and stiffness) act on the same soft mode that couples the sites. With quadratic landscapes, different types of ligand perturbations can drive cooperativity; applying a force results in a conformational change while stiffening changes the magnitude of fluctuations. Numerical values of H , \mathbf{u}_a , \mathbf{u}_b are given in the Appendix.

(IF) mechanism: ligands induce a conformational change through applying a force, each of the energy landscapes has a single minimum, ligand binding results in the translation of the minimum and there is a notion of a direct physical coupling between sites, here mediated through the soft modes.

Recent work has shown that linear elastic networks can be optimized for long-range allosteric tasks by varying the stiffness of the bonds [20, 21, 25, 31, 32, 36]. These models operate on the induced fit mechanism: an applied force or displacement of a few beads induces strain along one or several soft modes spanning the network, connecting a distant site.

Next, we consider second order ligand perturbations ($f_a = f_b = 0$, giving $V_a(\mathbf{r}) = \frac{1}{2}k_a(\mathbf{u}_a^\top \mathbf{r})^2$ and $V_b(\mathbf{r}) = \frac{1}{2}k_b(\mathbf{u}_b^\top \mathbf{r})^2$), thereby purely stiffening binding sites. In terms of proteins, this may correspond to binding a ligand that perfectly fits the geometry of the binding sites thereby not causing a change in conformation. In this case, the cooperativity computes to

$$\Delta\Delta F = -\frac{T}{2} \log \left(1 - \frac{k_a k_b (\mathbf{u}_a^\top H + \mathbf{u}_b) ^2}{(1 + k_a \mathbf{u}_a^\top H + \mathbf{u}_a)(1 + k_b \mathbf{u}_b^\top H + \mathbf{u}_b)} \right). \quad (12)$$

When both ligands stiffen (or soften) $k_a k_b > 0$ cooperativity can only be positive and requires the term $\mathbf{u}_a^\top H + \mathbf{u}_b$ to be non-zero. This indicates that soft modes must couple binding sites and that ligand binding must stiffen the same soft modes. This corresponds to the dynamic (or entropic) mechanism proposed by Cooper and Dryden [26] and studied extensively in minimal model and elastic networks by McLeish and colleagues [19, 27]. Additionally, this dynamics mechanism has been considered in a 1D model of allostery in DNA [34]. Negative cooperativity can occur when ligand binding stiffens one site but softens the other $k_a k_b < 0$. Regardless of sign, this cooperativity is purely entropic, $\Delta\Delta F = -T\Delta\Delta S$.

Both the induced fit (force) and dynamic (stiffness) mechanisms operate on the soft mode principle—binding sites coupled through soft normal modes—the difference lies in the details of the ligand binding interaction. In the general case, the ligand perturbations can be composed of both force and stiffness, however, the cooperativity does not take a simple analytical form (Methods). We graphically represent $\Delta\Delta F$ for the model under a range of ligand stiffnesses $k = k_a = k_b$ and forces $f = f_a = f_b$. Fig. 2A shows two regions of cooperativity, one where force dominates, corresponding to the induced fit mechanism, and the other where stiffness dominates corresponding to the dynamic mechanism.

While these two mechanisms operate on the same soft mode principle, physical features differ. This is apparent when representing the change in the mean conformation between the apo (00) and doubly bound (11) conditions, $\Delta\langle\mathbf{r}\rangle = \|\langle\mathbf{r}\rangle_{11} - \langle\mathbf{r}\rangle_{00}\|$ (here the subscript of the angle brackets denotes the ligation condition in which the average is taken). A conformational change occurs in the induced fit regime (Fig. 2B). The other regime recapitulates the “allostery without a conformational change” feature of dynamic allostery. However, this regime shows large changes in root mean squared fluctuations $\Delta\text{Var}(\mathbf{r}) = \left| \sqrt{\langle\mathbf{r}^2\rangle_{11} - \langle\mathbf{r}\rangle_{11}^2} - \sqrt{\langle\mathbf{r}^2\rangle_{00} - \langle\mathbf{r}\rangle_{00}^2} \right|$ upon binding of both ligands (Fig. 2C).

Bistable Models

What new mechanisms of cooperativity are possible when the landscape has multiple states? The calculation above showed that when minima are separated in conformational space ($\mathbf{u}_a^\top \mathbf{R}_i \neq \mathbf{u}_a^\top \mathbf{R}_j$ and $\mathbf{u}_b^\top \mathbf{R}_i \neq \mathbf{u}_b^\top \mathbf{R}_j$, for at least on pair states i, j), the free energy surface \tilde{F} is non separable and there is potential for cooperativity. To explore this, we minimally extend (10) to introduce

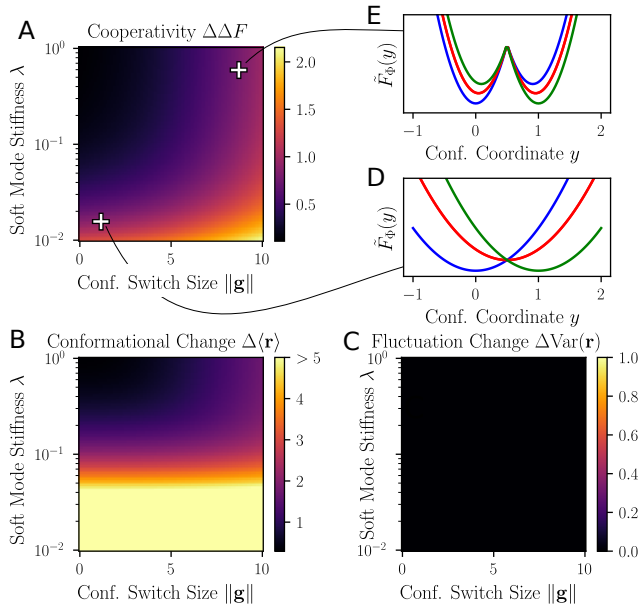


FIGURE 3. A bistable landscape offers two mechanisms of cooperativity. (A) cooperativity $\Delta\Delta F$, (B) mean conformational change upon ligand binding $\Delta\langle\mathbf{r}\rangle$, and (C) change in the magnitude of fluctuations upon ligand binding $\Delta\text{Var}(\mathbf{r})$ are plotted for a landscape with a bistability of strength $\|\mathbf{g}\|$ and a mode that couples bindings sites of stiffness λ . Ligand binding is treated as an applied force. (D) The free energy along the conformational change coordinate, $\tilde{F}_{\sigma_a\sigma_b}^{\Phi}(\phi)$, for the system located at the lower left + mark in (A) for the four ligation conditions. In this regime, the conformational switch mechanism is observed. (E) $\tilde{F}_{\sigma_a\sigma_b}^{\Phi}(\phi)$ for the system at the upper right + mark of (A) for the four ligation conditions. In this regime, the induced fit mechanism is observed. Numerical values of $H, \mathbf{g}, \mathbf{h}, \mathbf{u}_a, \mathbf{u}_b, f_a, f_b$ are given in the Appendix.

two-basins while retaining analytical tractability,

$$U_{\text{bi}}(\mathbf{r}) = \frac{1}{2}\mathbf{r}^{\top}H\mathbf{r} - |\mathbf{g}^{\top}\mathbf{r}| - \mathbf{h}^{\top}\mathbf{r}. \quad (13)$$

In this extension, bistability is introduced through the absolute value term with minima at $\mathbf{R}_1 = H^+(\mathbf{h} + \mathbf{g})$ and $\mathbf{R}_2 = H^+(\mathbf{h} - \mathbf{g})$. Each minimum retains a quadratic basin with curvature H , and an additional linear term $\mathbf{h}^{\top}\mathbf{r}$ controls the energy of one minimum relative to the other.

When a ligand applies a force ($V_a(\mathbf{r}) = -f_a\mathbf{u}_a^{\top}\mathbf{r}$, $V_b(\mathbf{r}) = -f_b\mathbf{u}_b^{\top}\mathbf{r}$), the cooperativity takes a lengthy analytical form. However, the basic principles are seen in the zero temperature limit where the free energy converges to the ground state energy. In this case the ground state cooperativity is,

$$\begin{aligned} \Delta\Delta E &= f_a f_b \mathbf{u}_a^{\top} H^+ \mathbf{u}_b \\ &+ \left| (f_a \mathbf{u}_a + f_b \mathbf{u}_b + \mathbf{h})^{\top} H^+ \mathbf{g} \right| + \left| \mathbf{h}^{\top} H^+ \mathbf{g} \right| \\ &- \left| (f_a \mathbf{u}_a + \mathbf{h})^{\top} H^+ \mathbf{g} \right| - \left| (f_b \mathbf{u}_b + \mathbf{h})^{\top} H^+ \mathbf{g} \right|. \end{aligned} \quad (14)$$

The most important feature is that cooperativity has two components : an induced fit term identical to (11) and terms that depend on the conformational switch parameter \mathbf{g} . These terms describe a mechanism in which the forces $f_a\mathbf{u}_a$ and $f_b\mathbf{u}_b$ communicate indirectly by both coupling to the bistable switch \mathbf{g} . Since the cooperativity scales with the bistable parameter \mathbf{g} the cooperativity can be arbitrarily large, irrespective of the strength of the perturbations. The conformational switch contribution is maximized when one minimum has initially lower energy and the ligand forces push the system to stabilize the other minimum. Conversely, negative cooperativity emerges when initially the minima have equal energy and the ligand forces push the system in opposite directions.

In Fig. 3A, we show the cooperativity at nonzero temperature ($T = 1$) of a system with a mode that couples binding sites with stiffness λ and conformational switch with magnitude $\|\mathbf{g}\|$ under conditions where ligands apply a force. As in the zero temperature expression, cooperativity can be achieved through the soft mode principle (3A bottom left), the MWC principle through a conformational switch (3A top right), or a combination of the two for increased cooperativity. When cooperativity emerges solely from the conformational switch (no soft mode contribution), the system can be written exactly as an MWC model (Methods).

Introducing a collective variable (CV) Φ that measures the projection of a conformation \mathbf{r} along the conformational change $\Delta\mathbf{R} = \langle\mathbf{r}\rangle_{11} - \langle\mathbf{r}\rangle_{00}$,

$$\Phi(\mathbf{r}) = \frac{\Delta\mathbf{R}}{\|\Delta\mathbf{R}\|} \cdot (\mathbf{r} - \langle\mathbf{r}\rangle_{00}) \quad (15)$$

we can compute free energy surfaces

$$\tilde{F}_{\sigma_a\sigma_b}^{\Phi}(\phi) = -\frac{1}{\beta} \log \left[\int d\mathbf{r} \delta(\Phi(\mathbf{r}) - \phi) e^{-\beta U_{\sigma_a\sigma_b}(\mathbf{r})} \right] \quad (16)$$

for the systems located at the bottom left (Fig. 3D) and upper right (Fig. 3E), marked as ‘+’ in Fig. 3A. Here, $U_{\sigma_a\sigma_b} = U_{\text{bi}} - \sigma_a f_a \mathbf{u}_a^{\top} \mathbf{r} - \sigma_b f_b \mathbf{u}_b^{\top} \mathbf{r}$. These 1d landscapes recapitulate the cartoon landscapes often drawn to graphically distinguish the induced fit and conformational switch mechanisms [22, 37–40]. Both mechanisms are underpinned by a conformational change (Fig. 3B) and have no ‘‘dynamical’’ change as shown by unchanged fluctuations upon ligand binding Fig. 3C.

An interesting distinction between these two mechanisms is how they scale with the magnitude of the ligand forces. With $f_a = f_b = f$, $g = \|\mathbf{g}\|$, and taking $\mathbf{h} = -f(\mathbf{u}_a + \mathbf{u}_b)/2$, we find that the induced fit component scales as $\kappa^{-1}f^2$ while the conformational switch component scales as $\kappa^{-1}gf$, where κ is an effective spring constant. These results suggest that the conformational switch mechanism is the best option when ligand binding imposes a subtle effect such as when the ligand closely fits the geometry of the binding site.

Many previous physical models used to explain allosteric cooperativity use a conformational switch mechanism.

These models include elastic networks where the conformational switch is explicitly added [23], or elastic networks where the conformational switch emerges through an evolutionary selection for cooperativity [25]. Alternatively, physical models whose constituting elements are themselves switch-like, such as spin models, operate on the conformational switch mechanism [24]. Upon ligand binding, an extended networks of tightly interacting spins flip orientation in a two-state way. Many coarse-grained models used to study allosteric features other than cooperativity have a double (or multi) basin energy landscape by design [41–46] and display conformational switch-like behavior.

Order-disorder Models

Bistable landscapes achieve cooperativity partly because spatially distinct minima make the free energy surface \tilde{F} non-separable. However, non-separability can be achieved even when minima overlap ($\mathbf{R}_i = \mathbf{R}_j$ for all pairs of states i, j) if the magnitude of fluctuations, specifically at the binding sites, differ between states, $\mathbf{u}_b H_i^+ \mathbf{u}_b \neq \mathbf{u}_b H_j^+ \mathbf{u}_b$ for at least one pair of states i, j . This condition occurs in systems with an order-disorder transition where the ordered state is low energy and low entropy and the disorder is high energy and high entropy. In proteins, global folding is one such transition: the native state is enthalpically stable and lower entropy than the unfolded state [47]. However, more subtle transitions exist, including partial or local folding [48, 49] as well as transitions between a compact yet disorder molten globule and a well-packed native states [50].

As a minimal potential that captures these features, we represent the ordered state with U_{quad} and explicitly add another potential to describe the disordered state,

$$U_{\text{dis}}(\mathbf{r}) = \frac{1}{2} \mathbf{r}^\top H_{\text{dis}} \mathbf{r} + \epsilon_{\text{dis}}. \quad (17)$$

Here $\epsilon_{\text{dis}} > 0$ represents the change in energy from breaking interactions between residues in the ordered state. To describe the high conformational entropy of the disordered state we consider $\|H_{\text{dis}}\| \ll \|H\|$. This choice of model is dictated by simplicity and analytical tractability. The two states are integrated in a free energy landscape with,

$$F_{\text{q,d}}(\mathbf{r}) = -\beta^{-1} \log \left[e^{-\beta U_{\text{quad}}(\mathbf{r})} + e^{-\beta U_{\text{dis}}(\mathbf{r})} \right]. \quad (18)$$

Since the ordered and disordered state have different entropies, ligand interactions that modulate the entropy have the greatest effect. For this reason, we consider the case where ligand binding changes the stiffness of the system, $V_a(\mathbf{r}) = k_a(\mathbf{u}_a^\top \mathbf{r})^2$, $V_b(\mathbf{r}) = k_b(\mathbf{u}_b^\top \mathbf{r})^2$.

We graphically analyze an order-disorder landscape where the native state curvature H has one mode that couples binding sites with stiffness λ and an energy difference of ϵ_{dis} . We take the curvature of the disordered

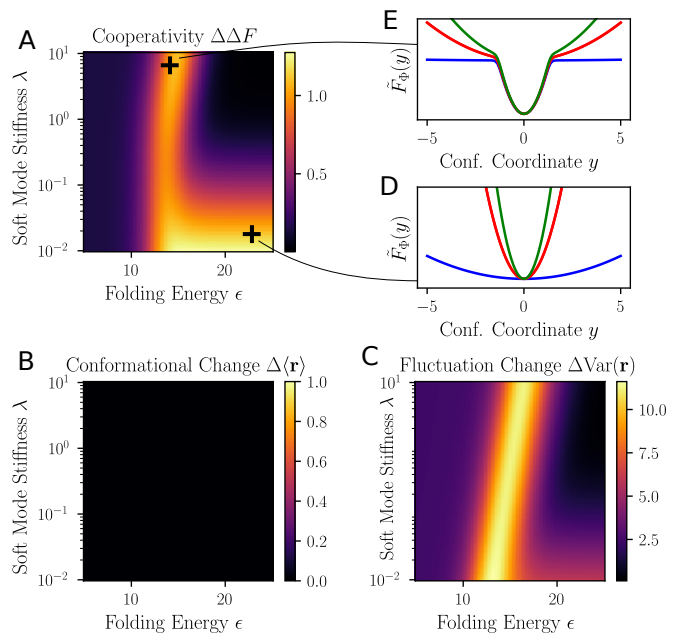


FIGURE 4. Two-state order-disorder landscapes offer two mechanisms of cooperativity. (A) The cooperativity $\Delta\Delta F$, (B) mean conformational change upon ligand binding $\Delta\langle\mathbf{r}\rangle$, (C) change in the magnitude of fluctuations upon ligand binding $\Delta\text{Var}(\mathbf{r})$, for an order-disorder model with energy difference ϵ_{dis} and a mode in the ordered state that couples bindings sites with stiffness λ . (D) Free energy along a conformational coordinate, $\tilde{F}_{\sigma_a\sigma_b}(\phi)$, for the system located at the lower right + mark in (A) for the four ligation conditions. In this regime, the dynamics mechanism is observed. (E) $\tilde{F}_{\sigma_a\sigma_b}(\phi)$ for the system at the upper center + mark of (A) for the four ligation conditions. In this regime, the order-disorder mechanism is observed. For these landscapes, $U_{\sigma_a\sigma_b} = F_{\text{q,d}} - \sigma_a k_a (\mathbf{u}_a^\top \mathbf{r})^2 - \sigma_b k_b (\mathbf{u}_b^\top \mathbf{r})^2$ in (16), and we set $\Delta\mathbf{R}$ of (15) to be the soft mode since there is no conformational change upon binding. The parameter values for this model are given in the Appendix.

state to be isotropic, $H_{\text{dis}} \propto I$ (this implies $\mathbf{u}_a^\top H_{\text{dis}}^+ \mathbf{u}_b = 0$). Fig. 4A shows the cooperativity of this minimal system. At low values of ϵ_{dis} the model is in the disordered state for all ligation conditions and no cooperativity occurs. At high values of ϵ_{dis} the model occupies the ordered state for all ligation conditions and cooperativity only occurs through the dynamic mechanism when the mode is soft. At intermediate values of ϵ_{dis} the model is disordered in the absence of ligands and ordered in their presence and cooperativity occurs even in the absence of a soft mode. When cooperativity emerges solely from the transitions between the ordered and disordered states (no soft mode contribution), the system can be written exactly as an MWC model (Methods). The transition is coupled with binding due to the larger decrease in entropy of the disordered state compared to the ordered state when ligands stiffen.

As with bistable landscapes, order-disorder landscapes enable a mechanism of cooperative binding distinct from

the one enabled by the soft mode principle. In both the dynamic mechanism and order-disorder mechanism, the mean structure is unchanged upon ligand binding (Fig. 4B, a result of the landscape being symmetric around the minimum) but the magnitude of the fluctuations is greatly reduced, concomitantly the effective rigidity increases and entropy decreases. The similar response to ligand binding has implications for experiments that attempt to resolve the mechanisms of cooperativity by measurements of dynamics and entropy before and after ligand binding.

In the limit where the ordered state is very stable (large ϵ_{dis}), the disordered state is irrelevant and we recover the dynamic mechanism that we described for a single state, as shown in Fig. 4D by the 1d free energy surface $\tilde{F}_{\sigma_a \sigma_b}^{\Phi}(\phi)$, plotted for the system located at the lower right ‘+’ mark of Fig. 4A. When the ordered state is only moderately stable, however, we obtain a qualitatively different picture, as shown in Fig. 4E by the 1d energy landscape of the system located at the upper ‘+’ mark of Fig. 4A. There the curvature of the ordered state is relatively unchanged, yet the curvature, and thus the free energy, of the disordered state increases significantly.

Hilser and Thompson proposed a thermodynamic model of allostery in which different states are interpreted to be folded or unfolded (discussed further in the discussion) [9]. However, to our knowledge, there have been no physical models that demonstrate how allosteric cooperativity can be enabled through any order-disorder transition.

Distinguishing mechanism in proteins

The energy landscapes of proteins are complicated and largely unknown, raising the question of how to distinguish the underlying physical principle, especially when, the relevant states may not be known. In thermodynamic systems, a state is associated with a minimum of a free energy surface over a set of collective variables. Measuring free energy surfaces in macromolecules through experiment is possible [51, 52] however molecular dynamics simulations provide a more accessible approach. Here we propose how the mechanisms of allostery of a protein may be distinguished with a combination of two simple CVs.

The CV Φ (15) identifies one minimum for the induced fit mechanism (Fig. 3D) and two minima for the conformational switch mechanism (Fig. 3E). However, it fails to identify two minima for the order-disorder mechanism, because there is no change in the mean conformation but rather a transition in the magnitude of fluctuations about the mean conformation. To capture the order-disorder changes, we propose a CV, Ψ , that measures root mean squared fluctuations around a set of conformations (see (71) for definition). As different mechanisms can operate in combination, measuring the free energy surface over Φ that captures changes along a conformational direc-

tion and Ψ that captures the order can help reveal the relevant mechanisms. In Fig. 5 we plot Monte Carlo estimates of the free energy surface over these CVs for the unbound ($\tilde{F}_{00}^{\Phi\Psi}(\phi, \psi)$, top row) and doubly bound condition ($\tilde{F}_{11}^{\Phi\Psi}(\phi, \psi)$, bottom row). Here ϕ identifies a value of Φ and ψ identifies a value of Ψ , see (72). Columns a, b, c, and d show the induced fit, conformational switch, dynamics, and order-disorder cases, respectively. While we consider simple cases of a minimal model, the same approach can be applied to more detailed molecular models of proteins whose allosteric mechanism is not well characterized.

DISCUSSION

Previous work has stressed the importance of different physical features in allostery: conformational changes, dynamical changes, multiple preexisting conformational states, soft normal modes, intrinsic disorder, folding, etc. The diversity of these features, and the varying levels of abstraction in the models that implement them, have made resolving fundamental principles from superficial detail difficult. In this work, we presented a physical framework from which the essential conditions for allosteric cooperativity can be identified.

Our main result is that cooperativity only emerges when the system satisfies one (or a combination) of two physical principles. The first is a soft mode principle where, within a single state, binding sites are coupled through soft normal modes and ligand binding to the different sites perturb the same modes. The second is the MWC principle which occurs when the system has multiple states with different affinities for the ligands. Upon binding, the system undergoes a switch-like transition between the states. While the MWC principle can be fully defined at the level of discrete thermodynamic states, the soft-mode principle requires a physical description of the energy landscape around a minimum and is not captured in thermodynamic models.

We show that each principle can have various physical implementations. Both the induced fit and dynamic mechanisms operate on the soft mode principle, with the difference between them lying in how ligand binding perturbs the soft mode—either by applying a force or by stiffening the modes. The conformational switch mechanism (sometimes called population shift [22]), where the two states are different conformations, and the order-disorder mechanism, where the two states have different magnitudes of fluctuations, both operate on the MWC principle. This framework unifies the different mechanisms of allostery which are often discussed in isolation, leading to a simpler understanding of allostery.

The cases we have considered are only four simple limits to illustrate the contribution of isolated features. More complicated potentials may result in mechanisms that may appear different, yet will still depend on the two physical principles as the calculation of separability

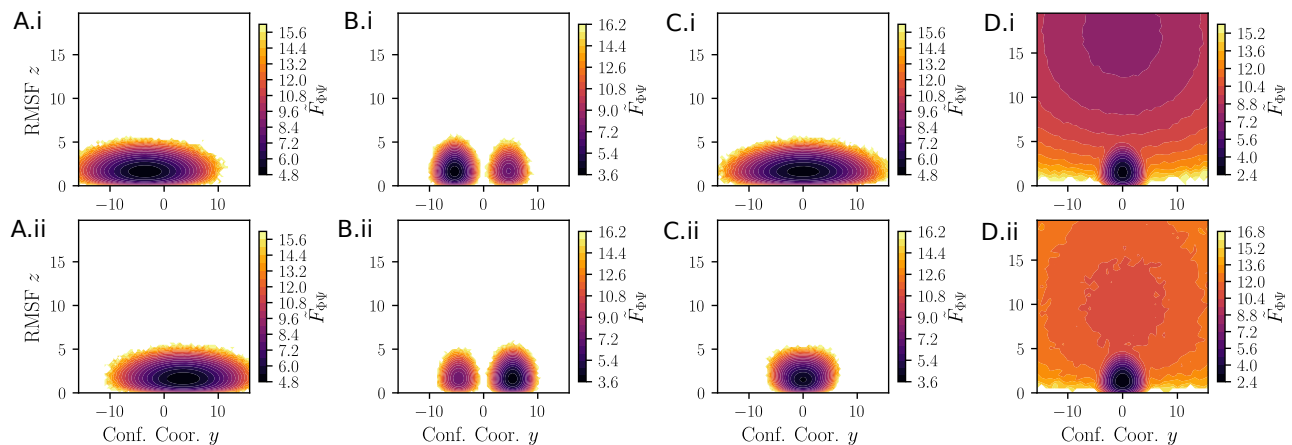


FIGURE 5. Free energy surfaces for different mechanisms of cooperativity. Panels show $\tilde{F}_{00}^{\Phi\Psi}(\phi, \psi)$ (for top row) or $\tilde{F}_{11}^{\Phi\Psi}(\phi, \psi)$ (for bottom row) calculated from an equilibrium Monte Carlo sample for cases that use the (A) induced fit (B) conformational switch (C) dynamic (D) order-disorder mechanisms (Appendix). Panels labeled with “i” show the unbound condition, and panels with “ii” show the doubly bound condition. Free energy surfaces along simple CVs that measure conformational changes Φ disorder Ψ can distinguish different mechanisms of cooperativity and can be used for far more detailed molecular models of proteins.

assumed generic protein and ligand binding potentials.

Limitations of model : We have considered a purely thermodynamic definition of allostery (i.e. cooperativity). As a result, kinetic and non-equilibrium features, such as the rate of crossing a barrier [53, 54] or the temporal order molecular events [42, 55], are not described.

Our model is defined at the level of the energy landscape and there is no inherent notion of geometry. As a result, we can not make predictions of structural features such as how the cooperativity should scale with the distance between binding sites or the size of the protein [21, 23, 34].

In terms of the forms of the energy landscapes, we made two notable assumptions. For analytical simplicity, we assumed that the ligand potentials act along a single mode of each binding site ((3)). However, in the supplement we relax this assumption by considering arbitrary potentials V_a, V_b , and show that the same two principles for cooperativity emerge. The second assumption is that a protein energy landscape can be well approximated by a multi-basin landscape (7). This approach is physically justified around minima and is commonly applied to protein landscapes [41, 56].

Implication for experiments How can this theoretical work guide experimental and computational studies of al-

lostery in proteins? One implication for applied research is that the common method of characterizing mechanisms by measuring conformations and fluctuations with and without ligand bound may not distinguish the underlying physical principles. For instance, allosteric proteins that do not exhibit conformational changes upon binding are often referred to as examples of “dynamic” [57], or “dynamically driven” [58] allostery. A common feature in these cases is that ligand binding stiffens a previously flexible protein. However, both the dynamic mechanism and the order-disorder mechanism, share this characteristic, and it is unclear which principle is at play in these proteins. To our knowledge, this distinction has not been addressed in previous studies, highlighting the importance of theoretical analysis in understanding allostery.

ACKNOWLEDGMENTS

We thank Kabir Husain, and members of the Ranganathan and Rivoire Labs for helpful discussions. R.R. and O.R. are grateful for funding from the FACCTS program of the France Chicago Center. R.R. acknowledges support from NIH RO1GM12345 and RO1GM141697, the University of Chicago, and O.R. from ANR-21-CE45-0033 and ANR-22-CE06-0037.

-
- [1] J. Monod, J.-P. Changeux, and F. Jacob, Allosteric proteins and cellular control systems, *Journal of molecular biology* **6**, 306 (1963).
 [2] L. T. May, K. Leach, P. M. Sexton, and A. Christopoulos, Allosteric modulation of g protein-coupled receptors,

- Annu. Rev. Pharmacol. Toxicol.* **47**, 1 (2007).
 [3] P. Pellicena and J. Kuriyan, Protein-protein interactions in the allosteric regulation of protein kinases, *Current opinion in structural biology* **16**, 702 (2006).
 [4] J. Monod, J. Wyman, and J.-P. Changeux, On the nature

- of allosteric transitions : a plausible model, *J Mol Biol* **12**, 88 (1965).
- [5] D. Koshland Jr, G. Nemethy, and D. Filmer, Comparison of experimental binding data and theoretical models in proteins containing subunits, *Biochemistry* **5**, 365 (1966).
- [6] J. Herzfeld and H. E. Stanley, A general approach to cooperativity and its application to the oxygen equilibrium of hemoglobin and its effectors, *Journal of molecular biology* **82**, 231 (1974).
- [7] M. Eigen, New looks and outlooks on physical enzymology, *Quarterly reviews of biophysics* **1**, 3 (1968).
- [8] W. A. Eaton, E. R. Henry, J. Hofrichter, S. Bettati, C. Viappiani, and A. Mozzarelli, Evolution of allosteric models for hemoglobin, *IUBMB life* **59**, 586 (2007).
- [9] V. J. Hilser and E. B. Thompson, Intrinsic disorder as a mechanism to optimize allosteric coupling in proteins, *Proceedings of the National Academy of Sciences* **104**, 8311 (2007).
- [10] L. Zhang, M. Li, and Z. Liu, A comprehensive ensemble model for comparing the allosteric effect of ordered and disordered proteins, *PLOS Computational Biology* **14**, e1006393 (2018).
- [11] O. Yifrach and A. Horovitz, Nested cooperativity in the atpase activity of the oligomeric chaperonin groel, *Biochemistry* **34**, 5303 (1995).
- [12] Z. Liu, T. G. Gillis, S. Raman, and Q. Cui, A parameterized two-domain thermodynamic model explains diverse mutational effects on protein allostery, *Elife* **12**, RP92262 (2024).
- [13] L. Ma and Q. Cui, Activation mechanism of a signaling protein at atomic resolution from advanced computations, *Journal of the American Chemical Society* **129**, 10261 (2007).
- [14] K. Arora and C. L. Brooks III, Large-scale allosteric conformational transitions of adenylate kinase appear to involve a population-shift mechanism, *Proceedings of the National Academy of Sciences* **104**, 18496 (2007).
- [15] L. Li, V. N. Uversky, A. K. Dunker, and S. O. Meroueh, A computational investigation of allostery in the catabolite activator protein, *Journal of the American Chemical Society* **129**, 15668 (2007).
- [16] M. M. Tirion, Large amplitude elastic motions in proteins from a single-parameter, atomic analysis, *Physical review letters* **77**, 1905 (1996).
- [17] K. Hinsen, Analysis of domain motions by approximate normal mode calculations, *Proteins : Structure, Function, and Bioinformatics* **33**, 417 (1998).
- [18] A. R. Atilgan, S. Durell, R. L. Jernigan, M. C. Demirel, O. Keskin, and I. Bahar, Anisotropy of fluctuation dynamics of proteins with an elastic network model, *Biophysical journal* **80**, 505 (2001).
- [19] T. C. McLeish, T. Rodgers, and M. R. Wilson, Allostery without conformation change : modelling protein dynamics at multiple scales, *Physical biology* **10**, 056004 (2013).
- [20] S. Dutta, J.-P. Eckmann, A. Libchaber, and T. Tlusty, Green function of correlated genes in a minimal mechanical model of protein evolution, *Proceedings of the National Academy of Sciences* **115**, E4559 (2018).
- [21] L. Yan, R. Ravasio, C. Brito, and M. Wyart, Principles for optimal cooperativity in allosteric materials, *Biophysical journal* **114**, 2787 (2018).
- [22] C.-J. Tsai and R. Nussinov, A unified view of “how allostery works”, *PLoS computational biology* **10**, e1003394 (2014).
- [23] R. Ravasio, S. M. Flatt, L. Yan, S. Zamuner, C. Brito, and M. Wyart, Mechanics of allostery : contrasting the induced fit and population shift scenarios, *Biophysical journal* **117**, 1954 (2019).
- [24] O. Rivoire, Parsimonious evolutionary scenario for the origin of allostery and coevolution patterns in proteins, *Physical Review E* **100**, 032411 (2019).
- [25] E. Rouviere, R. Ranganathan, and O. Rivoire, Emergence of single-versus multi-state allostery, *PRX Life* **1**, 023004 (2023).
- [26] A. Cooper and D. Dryden, Allostery without conformational change : a plausible model, *European Biophysics Journal* **11**, 103 (1984).
- [27] R. J. Hawkins and T. C. McLeish, Coarse-grained model of entropic allostery, *Physical review letters* **93**, 098104 (2004).
- [28] V. J. Hilser, J. O. Wrabl, and H. N. Motlagh, Structural and energetic basis of allostery, *Annual review of biophysics* **41**, 585 (2012).
- [29] W. Zheng, B. R. Brooks, and D. Thirumalai, Low-frequency normal modes that describe allosteric transitions in biological nanomachines are robust to sequence variations, *Proceedings of the National Academy of Sciences* **103**, 7664 (2006).
- [30] C. Xu, D. Tobi, and I. Bahar, Allosteric changes in protein structure computed by a simple mechanical model : hemoglobin t-r2 transition, *Journal of molecular biology* **333**, 153 (2003).
- [31] J. W. Rocks, N. Pashine, I. Bischofberger, C. P. Goodrich, A. J. Liu, and S. R. Nagel, Designing allostery-inspired response in mechanical networks, *Proceedings of the National Academy of Sciences* **114**, 2520 (2017).
- [32] L. Yan, R. Ravasio, C. Brito, and M. Wyart, Architecture and coevolution of allosteric materials, *Proceedings of the National Academy of Sciences* **114**, 2526 (2017).
- [33] M. Hemery and O. Rivoire, Evolution of sparsity and modularity in a model of protein allostery, *Physical review E* **91**, 042704 (2015).
- [34] M. Segers, A. Voorspoels, T. Sakaue, and E. Carlon, Mechanisms of dna-mediated allostery, *Physical Review Letters* **131**, 238402 (2023).
- [35] I. A. Balabin, W. Yang, and D. N. Beratan, Coarse-grained modeling of allosteric regulation in protein receptors, *Proceedings of the National Academy of Sciences* **106**, 14253 (2009).
- [36] H. Flechsig, Design of elastic networks with evolutionary optimized long-range communication as mechanical models of allosteric proteins, *Biophysical journal* **113**, 558 (2017).
- [37] L. G. Ahuja, S. S. Taylor, and A. P. Kornev, Tuning the “violin” of protein kinases : The role of dynamics-based allostery, *IUBMB life* **71**, 685 (2019).
- [38] J. Guo and H.-X. Zhou, Protein allostery and conformational dynamics, *Chemical reviews* **116**, 6503 (2016).
- [39] N. Wu, M. Barahona, and S. N. Yaliraki, Allosteric communication and signal transduction in proteins, *Current Opinion in Structural Biology* **84**, 102737 (2024).
- [40] J.-P. Changeux and S. Edelstein, Conformational selection or induced fit ? 50 years of debate resolved, *F1000 biology reports* **3** (2011).
- [41] K.-i. Okazaki, N. Koga, S. Takada, J. N. Onuchic, and P. G. Wolynes, Multiple-basin energy landscapes for large-amplitude conformational motions of proteins :

- Structure-based molecular dynamics simulations, Proceedings of the National Academy of Sciences **103**, 11844 (2006).
- [42] K.-i. Okazaki and S. Takada, Dynamic energy landscape view of coupled binding and protein conformational change : induced-fit versus population-shift mechanisms, Proceedings of the National Academy of Sciences **105**, 11182 (2008).
- [43] W. Li, W. Wang, and S. Takada, Energy landscape views for interplays among folding, binding, and allostery of calmodulin domains, Proceedings of the National Academy of Sciences **111**, 10550 (2014).
- [44] M. D. Daily, G. N. Phillips Jr, and Q. Cui, Many local motions cooperate to produce the adenylate kinase conformational transition, Journal of molecular biology **400**, 618 (2010).
- [45] P. Maragakis and M. Karplus, Large amplitude conformational change in proteins explored with a plastic network model : adenylate kinase, Journal of Molecular Biology **352**, 807 (2005).
- [46] J.-W. Chu and G. A. Voth, Coarse-grained free energy functions for studying protein conformational changes : a double-well network model, Biophysical Journal **93**, 3860 (2007).
- [47] A. Šali, E. Shakhnovich, and M. Karplus, How does a protein fold?, nature **369**, 248 (1994).
- [48] L. Rundqvist, J. Å den, T. Sparrman, M. Wallgren, U. Olsson, and M. Wolf-Watz, Noncooperative folding of subdomains in adenylate kinase, Biochemistry **48**, 1911 (2009).
- [49] T. P. Schrank, D. W. Bolen, and V. J. Hilser, Rational modulation of conformational fluctuations in adenylate kinase reveals a local unfolding mechanism for allostery and functional adaptation in proteins, Proceedings of the National Academy of Sciences **106**, 16984 (2009).
- [50] O. Ptitsyn, Molten globule and protein folding, Advances in protein chemistry **47**, 83 (1995).
- [51] G. Hummer and A. Szabo, Free energy surfaces from single-molecule force spectroscopy, Accounts of chemical research **38**, 504 (2005).
- [52] N. C. Harris, Y. Song, and C.-H. Kiang, Experimental free energy surface reconstruction from single-molecule force spectroscopy using jarzynski's equality, Physical review letters **99**, 068101 (2007).
- [53] I. Graham and T. Duke, Dynamic hysteresis in a one-dimensional ising model : Application to allosteric proteins, Physical Review E **71**, 061923 (2005).
- [54] J. M. Robinson, Physical limits on computation by assemblies of allosteric proteins, Physical review letters **101**, 178104 (2008).
- [55] G. G. Hammes, Y.-C. Chang, and T. G. Oas, Conformational selection or induced fit : a flux description of reaction mechanism, Proceedings of the National Academy of Sciences **106**, 13737 (2009).
- [56] H. Klem, G. M. Hocky, and M. McCullagh, Size-and-shape space gaussian mixture models for structural clustering of molecular dynamics trajectories, Journal of chemical theory and computation **18**, 3218 (2022).
- [57] C. M. Petit, J. Zhang, P. J. Sapienza, E. J. Fuentes, and A. L. Lee, Hidden dynamic allostery in a pdz domain, Proceedings of the National Academy of Sciences **106**, 18249 (2009).
- [58] N. Popovych, S. Sun, R. H. Ebright, and C. G. Kalodimos, Dynamically driven protein allostery, Nature structural & molecular biology **13**, 831 (2006).

METHODS

Ligand Binding

Ligand binding is treated as a perturbation of U_p and acts only on the few beads that define each binding site. The first binding site, labeled site a , is defined by a set of beads \mathcal{B}_a and the ligand binding perturbation at this site is given by a function $V_a(\mathbf{r}_a)$ where $\mathbf{r}_a = \{\mathbf{r}_i\}$ for $i \in \mathcal{B}_a$. Similarly, the second binding site, b , is comprised of beads in \mathcal{B}_b , and the perturbation on this site is given by $V_b(\mathbf{r}_b)$ where $\mathbf{r}_b = \{\mathbf{r}_i\}$ for $i \in \mathcal{B}_b$. To describe allosteric cooperativity the sites are taken to have no overlap, $\mathcal{B}_a \cap \mathcal{B}_b = \emptyset$. To simplify notation in the main text, we write V_a and V_b as functions of all the degrees of freedom \mathbf{r} , with it implied that only the binding site degrees of freedom are acted upon.

At each binding site, we defined a linear collective variable (CV) : $X_a(\mathbf{r}) = \mathbf{u}_a^\top \mathbf{r}$, $X_b(\mathbf{r}) = \mathbf{u}_b^\top \mathbf{r}$. Here \mathbf{u}_a and \mathbf{u}_b are dimensionless unit vectors that have nonzero entries only on beads in \mathcal{B}_a and \mathcal{B}_b , respectively, and describe a single mode of each binding site. We assume that ligands interact with the protein only along the collective variables : $V_a(\mathbf{r}) = g_a(X_a(\mathbf{r}))$, $V_b(\mathbf{r}) = g_b(X_b(\mathbf{r}))$.

Multi-basin Free Energy Surface

Any energy landscape can be well approximated by the following free energy landscape,

$$F_p(\mathbf{r}) = -\frac{1}{\beta} \log \sum_{i=1}^n e^{-\beta \frac{1}{2}(\mathbf{r}-\mathbf{R}_i)^\top H_i(\mathbf{r}-\mathbf{R}_i) + \beta \epsilon_i}. \quad (19)$$

Each state is quadratic with curvature H_i , ground state \mathbf{R}_i and ground state energy ϵ_i . Substituting F_p for U_p in (5) and solving the integral, we find,

$$\tilde{Z}(x_a, x_b) = \frac{1}{h_0^{dN-2}} \int d\mathbf{r} \delta(\mathbf{u}_a^\top \mathbf{r} - x_a) \delta(\mathbf{u}_b^\top \mathbf{r} - x_b) e^{-\beta F_p(\mathbf{r})} \quad (20)$$

$$= \frac{1}{h_0^{dN-2}} \sum_{i=1}^n \int d\mathbf{r} \delta(\mathbf{u}_a^\top \mathbf{r} - x_a) \delta(\mathbf{u}_b^\top \mathbf{r} - x_b) e^{-\beta \frac{1}{2}(\mathbf{r}-\mathbf{R}_i)^\top H_i(\mathbf{r}-\mathbf{R}_i) + \beta \epsilon_i} \quad (21)$$

$$= \frac{1}{h_0^{dN-2}} \sum_{i=1}^n e^{-\beta \epsilon_i} \int ds_a e^{i2\pi s_a x_a} \int ds_b e^{i2\pi s_b x_b} \int d\mathbf{r} e^{-\frac{1}{2}\beta(\mathbf{r}-\mathbf{R}_i)^\top H_i(\mathbf{r}-\mathbf{R}_i) - i2\pi(s_a \mathbf{u}_a + s_b \mathbf{u}_b)^\top \mathbf{r}} \quad (22)$$

$$= \frac{1}{h_0^{dN-2}} \sum_{i=1}^n e^{-\beta \epsilon_i} \int ds_a e^{i2\pi s_a (x_a - \mathbf{u}_a^\top \mathbf{R}_i)} \int ds_b e^{i2\pi s_b (x_b - \mathbf{u}_b^\top \mathbf{R}_i)} \int d\mathbf{y}_i e^{-\frac{1}{2}\beta \mathbf{y}_i^\top H_i \mathbf{y}_i - i2\pi(s_a \mathbf{u}_a + s_b \mathbf{u}_b)^\top \mathbf{y}_i} \quad (23)$$

$$= h_0^2 \sum_{i=1}^n e^{-\beta \epsilon_i} \sqrt{\frac{(2\pi)^{dN}}{h_0^{2dN} \beta^{dN} \det(H_i)}} \int ds_a e^{i2\pi s_a (x_a - \mathbf{u}_a^\top \mathbf{R}_i)} \int ds_b e^{i2\pi s_b (x_b - \mathbf{u}_b^\top \mathbf{R}_i)} \left(e^{-2\pi^2 \beta^{-1} (s_a \mathbf{u}_a + s_b \mathbf{u}_b)^\top H_i^{-1} (s_a \mathbf{u}_a + s_b \mathbf{u}_b)} \right) \quad (24)$$

$$= h_0^2 \sum_{i=1}^n e^{-\beta \epsilon_i} \sqrt{\frac{(2\pi)^N}{h_0^{2dN} \beta^N \det(H_i)}} \int d\mathbf{s} e^{-2\pi \beta^{-1} \mathbf{s}^\top A_i \mathbf{s} + i2\pi \mathbf{x}_i^\top \mathbf{s}} \quad (25)$$

$$= \sum_{i=1}^n \sqrt{\frac{(2\pi)^{dN-2}}{h_0^{2(dN-2)} \beta^{dN-2} \det(A_i) \det(H_i)}} e^{-\beta(\frac{1}{2} \mathbf{x}_i^\top A_i^{-1} \mathbf{x}_i + \epsilon_i)} \quad (26)$$

$$(27)$$

On the third line, we write the delta functions in terms of their Fourier transforms, $\delta(t) = \int_{-\infty}^{\infty} e^{-i2\pi st} ds$. On the fourth line we used the substitution $\mathbf{y}_i = \mathbf{r} - \mathbf{R}_i$ and on the sixth line we introduced $\mathbf{s} = (s_a, s_b)$, $\mathbf{x}_i = (x_a - \mathbf{u}_a^\top \mathbf{R}_i, x_b - \mathbf{u}_b^\top \mathbf{R}_i)$ and

$$A_i = \begin{pmatrix} \mathbf{u}_a^\top H_i^+ \mathbf{u}_a & \mathbf{u}_a^\top H_i^+ \mathbf{u}_b \\ \mathbf{u}_a^\top H_i^+ \mathbf{u}_b & \mathbf{u}_b^\top H_i^+ \mathbf{u}_b \end{pmatrix}. \quad (28)$$

The free energy surface is,

$$\tilde{F}(x_a, x_b) = -\frac{1}{\beta} \log \left(\sum_{i=1}^n \sqrt{\frac{(2\pi)^{dN-2}}{h_0^{2(dN-2)} \beta^{dN-2} \det(A_i) \det(H_i)}} e^{-\beta(\frac{1}{2} \mathbf{x}_i^\top A_i^{-1} \mathbf{x}_i + \epsilon_i)} \right). \quad (29)$$

As before, cooperativity can only exist when the free energy surface is not separable, i.e. $\tilde{F}(x_a, x_b)$ can not be written as $\tilde{F}_a(x_a) + \tilde{F}_b(x_b)$. This happens when the off-diagonal entries of A^{-1} are zeros. The inverse of a symmetric 2×2 matrix is,

$$\begin{pmatrix} a & c \\ c & b \end{pmatrix}^{-1} = \frac{1}{ab - c^2} \begin{pmatrix} b & -c \\ -c & a \end{pmatrix}, \quad (30)$$

and so the condition for separability is,

$$\frac{-\mathbf{u}_a^\top H_i^+ \mathbf{u}_b}{\mathbf{u}_a^\top H_i^+ \mathbf{u}_a \mathbf{u}_b^\top H_i^+ \mathbf{u}_b - (2\mathbf{u}_a^\top H_i^+ \mathbf{u}_b)^2} \neq 0. \quad (31)$$

This condition happens when $\mathbf{u}_a^\top H_i^+ \mathbf{u}_b \neq 0$.

Scaling of cooperativity within a single basin

Here we show that $\Delta\Delta F \sim \mathbf{u}_a^\top H^+ \mathbf{u}_b$ when $\mathbf{u}_a^\top H^+ \mathbf{u}_b$ is small when there is a single basin ($n = 1$). The free energy surface when $n = 1$ simplifies to,

$$\tilde{F}(x_a, x_b) = \frac{1}{2} \mathbf{x}_1^\top A_1^{-1} \mathbf{x}_1 - \frac{1}{\beta} \log \left(\sqrt{\frac{(2\pi)^{dN-2}}{h_0^{2(dN-2)} \beta^{dN-2} \det(A_1) \det(H_1)}} \right) \quad (32)$$

Going forward we omit the subscripts on the Hessian and other parameters in this section, and we drop the constant term as it does not contribute to the cooperativity. Let $G = A^{-1}$ and $(x_a - \mathbf{u}_a^\top \mathbf{R}) = x_a - \mathbf{u}_a^\top \mathbf{R}$ and $(x_b - \mathbf{u}_b^\top \mathbf{R}) = x_b - \mathbf{u}_b^\top \mathbf{R}$. The quadratic terms can be written as,

$$\frac{1}{2} \mathbf{x}^\top A^{-1} \mathbf{x} = \frac{1}{2} G_{11} (x_a - \mathbf{u}_a^\top \mathbf{R})^2 + \frac{1}{2} G_{22} (x_b - \mathbf{u}_b^\top \mathbf{R})^2 + G_{12} (x_a - \mathbf{u}_a^\top \mathbf{R})(x_b - \mathbf{u}_b^\top \mathbf{R}). \quad (33)$$

The partition function (for which we omit the factor h_0^{-2} because it does not contribute to the cooperativity) becomes

$$Z_{\sigma_a \sigma_b} = \int dx_a e^{-\beta(\sigma_a g_a(x_a) + \frac{1}{2} G_{11} (x_a - \mathbf{u}_a^\top \mathbf{R})^2)} \int dx_b e^{-\beta(\sigma_b g_b(x_b) + \frac{1}{2} G_{22} (x_b - \mathbf{u}_b^\top \mathbf{R})^2)} e^{-\beta G_{12} (x_a - \mathbf{u}_a^\top \mathbf{R})(x_b - \mathbf{u}_b^\top \mathbf{R})}, \quad (34)$$

We are interested in the onset of cooperativity, so we consider the condition where $\mathbf{u}_a^\top H^+ \mathbf{u}_b$ is small (relative to $\mathbf{u}_a^\top H^+ \mathbf{u}_a$ and $\mathbf{u}_b^\top H^+ \mathbf{u}_b$). Since $G_{12} = -\mathbf{u}_a^\top H^+ \mathbf{u}_b / (\mathbf{u}_a^\top H^+ \mathbf{u}_a \mathbf{u}_b^\top H^+ \mathbf{u}_b - (\mathbf{u}_a^\top H^+ \mathbf{u}_b)^2)$, when $\mathbf{u}_a^\top H^+ \mathbf{u}_b$ is small, then G_{12} is small and $e^{-\beta G_{12} (x_a - \mathbf{u}_a^\top \mathbf{R})(x_b - \mathbf{u}_b^\top \mathbf{R})}$ can be approximated by a Taylor expansion of around $G_{12} = 0$ is,

$$e^{-\beta G_{12} (x_a - \mathbf{u}_a^\top \mathbf{R})(x_b - \mathbf{u}_b^\top \mathbf{R})} \approx 1 - \beta (x_a - \mathbf{u}_a^\top \mathbf{R})(x_b - \mathbf{u}_b^\top \mathbf{R}) G_{12} + \mathcal{O}(G_{12}^2) \quad (35)$$

Using this we get,

$$Z_{\sigma_a \sigma_b} = \int dx_a e^{-\beta(\sigma_a g_a(x_a) + \frac{1}{2} G_{11} (x_a - \mathbf{u}_a^\top \mathbf{R})^2)} \int dx_b e^{-\beta(\sigma_b g_b(x_b) + \frac{1}{2} G_{22} (x_b - \mathbf{u}_b^\top \mathbf{R})^2)} (1 - \beta (x_a - \mathbf{u}_a^\top \mathbf{R})(x_b - \mathbf{u}_b^\top \mathbf{R}) G_{12}) \quad (36)$$

$$= Z_{\sigma_a \sigma_b}^* - \beta G_{ab} \Omega_{\sigma_a \sigma_b} \quad (37)$$

where

$$Z_{\sigma_a \sigma_b}^* = \int dx_a e^{-\beta(\sigma_a g_a(x_a) + \frac{1}{2} G_{11} (x_a - \mathbf{u}_a^\top \mathbf{R})^2)} \int dx_b e^{-\beta(\sigma_b g_b(x_b) + \frac{1}{2} G_{22} (x_b - \mathbf{u}_b^\top \mathbf{R})^2)} \quad (38)$$

and

$$\Omega_{\sigma_a \sigma_b} = \int dx_a e^{-\beta(\sigma_a g_a(x_a) + \frac{1}{2} G_{11} (x_a - \mathbf{u}_a^\top \mathbf{R})^2)} \int dx_b e^{-\beta(\sigma_b g_b(x_b) + \frac{1}{2} G_{22} (x_b - \mathbf{u}_b^\top \mathbf{R})^2)} (x_a - \mathbf{u}_a^\top \mathbf{R})(x_b - \mathbf{u}_b^\top \mathbf{R}) \quad (39)$$

Using these, the fraction in the log of the cooperativity (2) gives,

$$\frac{Z_{10}Z_{01}}{Z_{00}Z_{11}} = \frac{(Z_{10}^* - \beta A_{ab}\Omega_{10})(Z_{01}^* - \beta A_{ab}\Omega_{01})}{(Z_{00}^* - \beta A_{ab}\Omega_{00})(Z_{11}^* - \beta A_{ab}\Omega_{11})} \quad (40)$$

$$= \frac{Z_{10}^*Z_{01}^* - \beta A_{ab}\Omega_{10}Z_{01}^* - \beta A_{ab}\Omega_{01}Z_{10}^* + \beta^2 A_{ab}^2\Omega_{10}\Omega_{01}}{Z_{00}^*Z_{11}^* - \beta A_{ab}\Omega_{00}Z_{11}^* - \beta A_{ab}\Omega_{11}Z_{00}^* + \beta^2 A_{ab}^2\Omega_{00}\Omega_{11}} \quad (41)$$

$$= \frac{Z_{10}^*Z_{01}^* - \beta A_{ab}(\Omega_{10}Z_{01}^* + \Omega_{01}Z_{10}^*)}{Z_{00}^*Z_{11}^* - \beta A_{ab}(\Omega_{00}Z_{11}^* + \Omega_{11}Z_{00}^*)}. \quad (42)$$

On the last line, we neglected the order G_{12}^2 terms. We also know that $Z_{10}^*Z_{01}^* = Z_{00}^*Z_{11}^*$. We use the relation,

$$\frac{a+b}{a+c} \approx 1 + \frac{b-c}{a} \quad (43)$$

which holds when $a \gg b$ and $a \gg c$.

$$\frac{Z_{10}Z_{01}}{Z_{00}Z_{11}} \approx 1 - \beta G_{12} \frac{\Omega_{10}Z_{01}^* + \Omega_{01}Z_{10}^* - \Omega_{00}Z_{11}^* - \Omega_{11}Z_{00}^*}{Z_{00}^*Z_{11}^*} \quad (44)$$

Now for the cooperativity when,

$$\Delta\Delta F = -\beta^{-1} \log \left(\frac{Z_{10}Z_{01}}{Z_{00}Z_{11}} \right) \approx G_{12} \frac{\Omega_{10}Z_{01}^* + \Omega_{01}Z_{10}^* - \Omega_{00}Z_{11}^* - \Omega_{11}Z_{00}^*}{Z_{00}^*Z_{11}^*} + \mathcal{O}(G_{12}^2) \quad (45)$$

Finally, this means that $\Delta\Delta F \sim \mathbf{u}_a^\top H^+ \mathbf{u}_b$ when small.

Derivation of Quadratic Cooperativities (11) and (12)

To compute cooperativities, ligand potential must be specified. We assume ligand binding affects a single mode of the systems local to each binding site (3), and we consider polynomial perturbations up to second order $g_a(x) = \frac{1}{2}k_a x^2 - f_a x$ and $g_b(x) = \frac{1}{2}k_b x^2 - f_b x$ (constant terms will not contribute to $\Delta\Delta F$ and are omitted). The full partition function becomes,

$$Z_{\sigma_a\sigma_b} = C \int dx_a e^{-\sigma_a \beta g_a(x_a)} \int dx_b e^{-\sigma_b \beta g_b(x_b)} e^{-\frac{1}{2}\beta \mathbf{x}^\top A^{-1} \mathbf{x}} \quad (46)$$

Here C is a constant that has the constant term of (32) folded into it. To compute the cooperativity (2) we need to compute the partition function for each binding condition. For the apo state ($\sigma_a, \sigma_b = 0, 0$) we find,

$$Z_{00} = C \int d\mathbf{x} e^{-\frac{1}{2}\beta \mathbf{x}^\top A^{-1} \mathbf{x}} = C \sqrt{\frac{(2\pi)^2}{\beta^2 \det(A^{-1})}} = C \frac{2\pi}{\beta} \sqrt{\mathbf{u}_a^\top H^+ \mathbf{u}_a \mathbf{u}_b^\top H^+ \mathbf{u}_b - (\mathbf{u}_a^\top H^+ \mathbf{u}_b)^2}. \quad (47)$$

When one ligand binds to the a site ($\sigma_a, \sigma_b = 1, 0$),

$$Z_{10} = C \int d\mathbf{x} e^{-\beta(\frac{1}{2}\mathbf{x}^\top A^{-1} \mathbf{x} + \frac{1}{2}k_a x_a^2 - f_a x_a)} \quad (48)$$

$$= C \int d\mathbf{x} e^{-\beta(\frac{1}{2}\mathbf{x}^\top (A^{-1} + k_a \mathbf{e}_1 \mathbf{e}_1^\top) \mathbf{x} - f_a \mathbf{e}_1^\top \mathbf{x}_a)} \quad (49)$$

$$= C \sqrt{\frac{(2\pi)^2}{\beta^2 \det(A^{-1} + k_a \mathbf{e}_1 \mathbf{e}_1^\top)}} e^{\frac{1}{2}\beta f_a^2 \mathbf{e}_1^\top (A^{-1} + k_a \mathbf{e}_1 \mathbf{e}_1^\top)^{-1} \mathbf{e}_1}. \quad (50)$$

Here $\mathbf{e}_1 = (1, 0)$ and later we will use $\mathbf{e}_2 = (0, 1)$. Using the Sherman-Morrison formula we find,

$$\mathbf{e}_1^\top (A^{-1} + k_a \mathbf{e}_1 \mathbf{e}_1^\top)^{-1} \mathbf{e}_1 = \frac{\mathbf{u}_a^\top H^+ \mathbf{u}_a}{1 + k_a \mathbf{u}_a^\top H^+ \mathbf{u}_a}. \quad (51)$$

Using the Matrix determinant lemma,

$$\det(A^{-1} + k_a \mathbf{e}_1 \mathbf{e}_1^\top) = \frac{1 + k_a \mathbf{u}_a H^+ \mathbf{u}_a}{\mathbf{u}_a H^+ \mathbf{u}_a \mathbf{u}_b H^+ \mathbf{u}_b - (\mathbf{u}_a H^+ \mathbf{u}_b)^2} \quad (52)$$

Similarly when one ligand binds to the b site ($\sigma_a, \sigma_b = 0, 1$), we find

$$Z_{10} = C \sqrt{\frac{(2\pi)^2}{\beta^2 \det(A^{-1} + k_b \mathbf{e}_2 \mathbf{e}_2^\top)}} e^{\frac{1}{2} \beta f_b^2 \mathbf{e}_2^\top (A^{-1} + k_b \mathbf{e}_2 \mathbf{e}_2^\top)^{-1} \mathbf{e}_2} \quad (53)$$

$$\mathbf{e}_2^\top (A^{-1} + k_b \mathbf{e}_2 \mathbf{e}_2^\top)^{-1} \mathbf{e}_2 = \frac{\mathbf{u}_b^\top H^+ \mathbf{u}_b}{1 + k_a \mathbf{u}_b^\top H^+ \mathbf{u}_b}. \quad (54)$$

$$\det(A^{-1} + k_b \mathbf{e}_2 \mathbf{e}_2^\top) = \frac{1 + k_b \mathbf{u}_b H^+ \mathbf{u}_b}{\mathbf{u}_a H^+ \mathbf{u}_a \mathbf{u}_b H^+ \mathbf{u}_b - (\mathbf{u}_a H^+ \mathbf{u}_b)^2} \quad (55)$$

When both sites are bound ($\sigma_a, \sigma_b = 1, 1$) the partition function becomes

$$Z_{11} = C \sqrt{\frac{(2\pi)^2}{\beta^2 \det(A^{-1} + k_a \mathbf{e}_1 \mathbf{e}_1^\top + k_b \mathbf{e}_2 \mathbf{e}_2^\top)}} e^{\frac{1}{2} \beta (f_a \mathbf{e}_1 + f_b \mathbf{e}_2)^\top (A^{-1} + k_a \mathbf{e}_1 \mathbf{e}_1^\top + k_b \mathbf{e}_2 \mathbf{e}_2^\top)^{-1} (f_a \mathbf{e}_1 + f_b \mathbf{e}_2)} \quad (56)$$

$$\begin{aligned} & (f_a \mathbf{e}_1 + f_b \mathbf{e}_2)^\top (A^{-1} + k_a \mathbf{e}_1 \mathbf{e}_1^\top + k_b \mathbf{e}_2 \mathbf{e}_2^\top)^{-1} (f_a \mathbf{e}_1 + f_b \mathbf{e}_2) = \\ & \frac{2\mathbf{u}_a^\top H^+ \mathbf{u}_b f_a f_b + \mathbf{u}_b^\top H^+ \mathbf{u}_b f_b^2 + \mathbf{u}_a^\top H^+ \mathbf{u}_a \mathbf{u}_b^\top H^+ \mathbf{u}_b f_b^2 k_a + \mathbf{u}_a^\top H^+ \mathbf{u}_a f_a^2 (1 + \mathbf{u}_b^\top H^+ \mathbf{u}_b k_b) - \mathbf{u}_a^\top H^+ \mathbf{u}_b^2 (f_b^2 k_a + f_a^2 k_b)}{1 + \mathbf{u}_b^\top H^+ \mathbf{u}_b k_b - \mathbf{u}_a^\top H^+ \mathbf{u}_b^2 k_a k_b + \mathbf{u}_a^\top H^+ \mathbf{u}_a (k_a + \mathbf{u}_b^\top H^+ \mathbf{u}_b k_a k_b)} \end{aligned} \quad (57)$$

$$\det(A^{-1} + k_a \mathbf{e}_1 \mathbf{e}_1^\top + k_b \mathbf{e}_2 \mathbf{e}_2^\top) = \frac{1 + k_a \mathbf{u}_a^\top H^+ \mathbf{u}_a + k_b \mathbf{u}_b^\top H^+ \mathbf{u}_b + k_a k_b (\mathbf{u}_a^\top H^+ \mathbf{u}_a \mathbf{u}_b^\top H^+ \mathbf{u}_b - (\mathbf{u}_a^\top H^+ \mathbf{u}_b)^2)}{\mathbf{u}_a^\top H^+ \mathbf{u}_a \mathbf{u}_b^\top H^+ \mathbf{u}_b - (\mathbf{u}_a^\top H^+ \mathbf{u}_b)^2} \quad (58)$$

And the full cooperativity becomes

$$\begin{aligned} \Delta \Delta F &= \frac{2f_a f_b \mathbf{u}_a^\top H^+ \mathbf{u}_b (1 + k_a \mathbf{u}_a^\top H^+ \mathbf{u}_a + k_b \mathbf{u}_b^\top H^+ \mathbf{u}_b + k_a k_b \mathbf{u}_a^\top H^+ \mathbf{u}_a \mathbf{u}_b^\top H^+ \mathbf{u}_b)}{2(1 + k_a \mathbf{u}_a^\top H^+ \mathbf{u}_a)(1 + k_b \mathbf{u}_b^\top H^+ \mathbf{u}_b)(1 + k_a \mathbf{u}_a^\top H^+ \mathbf{u}_a + k_b \mathbf{u}_b^\top H^+ \mathbf{u}_b + k_a k_b (\mathbf{u}_a^\top H^+ \mathbf{u}_a \mathbf{u}_b^\top H^+ \mathbf{u}_b + \mathbf{u}_a^\top H^+ \mathbf{u}_b^2))} \\ & \times \frac{-(\mathbf{u}_a^\top H^+ \mathbf{u}_b)^2 (k_a f_b^2 + k_b f_a^2 + \mathbf{u}_a^\top H^+ \mathbf{u}_a f_b^2 k_a^2 + \mathbf{u}_b^\top H^+ \mathbf{u}_b f_a^2 k_b^2)}{2(1 + k_a \mathbf{u}_a^\top H^+ \mathbf{u}_a)(1 + k_b \mathbf{u}_b^\top H^+ \mathbf{u}_b)(1 + k_a \mathbf{u}_a^\top H^+ \mathbf{u}_a + k_b \mathbf{u}_b^\top H^+ \mathbf{u}_b + k_a k_b (\mathbf{u}_a^\top H^+ \mathbf{u}_a \mathbf{u}_b^\top H^+ \mathbf{u}_b + (\mathbf{u}_a^\top H^+ \mathbf{u}_b)^2))} \\ & - \frac{1}{2\beta} \log \left(1 - \frac{k_a k_b (\mathbf{u}_a^\top H^+ \mathbf{u}_b)^2}{(1 + k_a \mathbf{u}_a^\top H^+ \mathbf{u}_a)(1 + k_b \mathbf{u}_b^\top H^+ \mathbf{u}_b)} \right). \end{aligned} \quad (59)$$

We see that when binding purely applies a force, the cooperativity reduces to (11).

$$\text{When } k_a = k_b = 0 \quad \rightarrow \quad \Delta \Delta F = f_a f_b \mathbf{u}_b^\top H^+ \mathbf{u}_b, \quad (60)$$

and when binding purely stiffens the cooperativity reduces to (12),

$$\text{When } f_a = f_b = 0 \quad \rightarrow \quad \Delta \Delta F = -\frac{1}{2\beta} \log \left(1 - \frac{k_a k_b (\mathbf{u}_a^\top H^+ \mathbf{u}_b)^2}{(1 + k_a \mathbf{u}_a^\top H^+ \mathbf{u}_a)(1 + k_b \mathbf{u}_b^\top H^+ \mathbf{u}_b)} \right). \quad (61)$$

A. Derivation of Conformational Switch Cooperativity (14)

Starting with the bistable energy landscape $U_{\text{bi}}(\mathbf{r})$ defined in (13) and ligand perturbation that apply forces, $V_a(\mathbf{r}) = f_a \mathbf{u}_a^\top \mathbf{r}$, $V_b(\mathbf{r}) = f_b \mathbf{u}_b^\top \mathbf{r}$, the energy landscape of each binding condition is,

$$U_{\sigma_a \sigma_b}(\mathbf{r}) = U_{\text{bi}}(\mathbf{r}) - \sigma_a f_a \mathbf{u}_a^\top \mathbf{r} - f_b \mathbf{u}_b^\top \mathbf{r}. \quad (62)$$

Each of these energies will have two minima if the following condition is met,

$$\mathbf{g}^\top H^+ (\mathbf{h} + \mathbf{f} - \mathbf{g}) < 0 < \mathbf{g}^\top H^+ (\mathbf{h} + \mathbf{f} + \mathbf{g}), \quad (63)$$

where $\mathbf{f} = \sigma_a f_a \mathbf{u}_a + \sigma_b f_b \mathbf{u}_b$. For a generic quadratic potential with an applied force $U(\mathbf{r}) = \mathbf{r}^\top H \mathbf{r} - \mathbf{f}^\top \mathbf{r}$ there will be a minimum at $\mathbf{r}_{\text{min}} = H^+ \mathbf{f}$ of energy $E = \min_{\mathbf{r}} U(\mathbf{r}) = -\frac{1}{2} \mathbf{f}^\top H^+ \mathbf{f}$. When there are two minima, they will have energies,

$$E_+ = -\frac{1}{2} (\mathbf{f} + \mathbf{h} + \mathbf{g})^\top H^+ (\mathbf{f} + \mathbf{h} + \mathbf{g}), \quad E_- = -\frac{1}{2} (\mathbf{f} + \mathbf{h} - \mathbf{g})^\top H^+ (\mathbf{f} + \mathbf{h} - \mathbf{g}) \quad (64)$$

The ground state energy is,

$$E = \min(E_+, E_-) = \frac{1}{2} (E_+ + E_- - |E_+ - E_-|) \quad (65)$$

$$= -\frac{1}{2} \mathbf{f}^\top H^+ \mathbf{f} - \frac{1}{2} \mathbf{h}^\top H^+ \mathbf{h} - \frac{1}{2} \mathbf{g}^\top H^+ \mathbf{g} - \mathbf{f}^\top H^+ \mathbf{h} - |\mathbf{f}^\top H^+ \mathbf{g} + \mathbf{h}^\top H^+ \mathbf{g}| \quad (66)$$

The cooperativity of the bistable landscape becomes,

$$\begin{aligned} \Delta \Delta E = & -\frac{1}{2} f_a^2 \mathbf{u}_a^\top H^+ \mathbf{u}_a - \frac{1}{2} \mathbf{h}^\top H^+ \mathbf{h} - \frac{1}{2} \mathbf{g}^\top H^+ \mathbf{g} - f_a \mathbf{u}_a^\top H^+ \mathbf{h} - |f_a \mathbf{u}_a^\top H^+ \mathbf{g} + \mathbf{h}^\top H^+ \mathbf{g}| \\ & - \frac{1}{2} f_b^2 \mathbf{u}_b^\top H^+ \mathbf{u}_b - \frac{1}{2} \mathbf{h}^\top H^+ \mathbf{h} - \frac{1}{2} \mathbf{g}^\top H^+ \mathbf{g} - f_b \mathbf{u}_b^\top H^+ \mathbf{h} - |f_b \mathbf{u}_b^\top H^+ \mathbf{g} + \mathbf{h}^\top H^+ \mathbf{g}| \\ & + \frac{1}{2} \mathbf{h}^\top H^+ \mathbf{h} + \frac{1}{2} \mathbf{g}^\top H^+ \mathbf{g} + |\mathbf{h}^\top H^+ \mathbf{g}| \\ & + \frac{1}{2} (f_a \mathbf{u}_a + f_b \mathbf{u}_b)^\top H^+ (f_a \mathbf{u}_a + f_b \mathbf{u}_b) + \frac{1}{2} \mathbf{h}^\top H^+ \mathbf{h} + \frac{1}{2} \mathbf{g}^\top H^+ \mathbf{g} + (f_a \mathbf{u}_a + f_b \mathbf{u}_b)^\top H^+ \mathbf{h} \\ & + |(f_a \mathbf{u}_a + f_b \mathbf{u}_b)^\top H^+ \mathbf{g} + \mathbf{h}^\top H^+ \mathbf{g}| \end{aligned} \quad (67)$$

$$\Delta \Delta E = f_a f_b \mathbf{u}_a^\top H^+ \mathbf{u}_b + |(f_a \mathbf{u}_a + f_b \mathbf{u}_b + \mathbf{h})^\top H^+ \mathbf{g}| + |\mathbf{h}^\top H^+ \mathbf{g}| - |(f_a \mathbf{u}_a + \mathbf{h})^\top H^+ \mathbf{g}| - |(f_b \mathbf{u}_b + \mathbf{h})^\top H^+ \mathbf{g}|. \quad (68)$$

B. Definitions of Quantities

Conformational Change : The conformational change is measured as the magnitude of the difference in the mean conformation with both ligand bound, $\langle \mathbf{r} \rangle_{11}$, and no ligand bound $\langle \mathbf{r} \rangle_{00}$,

$$\Delta \langle \mathbf{r} \rangle = \|\langle \mathbf{r} \rangle_{11} - \langle \mathbf{r} \rangle_{00}\|. \quad (69)$$

Fluctuation Change : To measure the change in the magnitude of the fluctuations around the mean conformation we measure the change in the RMSF upon binding both ligands,

$$\Delta \text{Var}(\mathbf{r}) = \left| \sqrt{\langle \mathbf{r}^2 \rangle_{11} - \langle \mathbf{r} \rangle_{11}^2} - \sqrt{\langle \mathbf{r}^2 \rangle_{00} - \langle \mathbf{r} \rangle_{00}^2} \right| \quad (70)$$

Here the subscripts on the angle brackets indicate the ligand binding condition for which the average is taken.

Disorder Collective Variable. Transitions such as folding are not well captured by a CV that measures changes along a single conformational direction such as Φ (15). Rather a CV that captures order-disorder transitions is needed and we propose the following modified RMSF CV,

$$\Psi(\mathbf{r}) = \left\| (\mathbf{r} - \langle \mathbf{r} \rangle_{00}) - \left((\mathbf{r} - \langle \mathbf{r} \rangle_{00}) \cdot \widehat{\Delta \mathbf{R}} \right) \widehat{\Delta \mathbf{R}} \right\|, \quad (71)$$

where $\widehat{\Delta\mathbf{R}} = \Delta\mathbf{R}/\|\Delta\mathbf{R}\|$. This CV measures the conformational deviations in directions other than $\Delta\mathbf{R}$. A 2d free energy surface in Φ and Ψ can capture conformational changes and order-disorder changes.

$$\tilde{F}_{\sigma_a\sigma_b}^{\Phi\Psi}(\phi, \psi) = -\frac{1}{\beta} \log \left(\frac{1}{h_0^{dN-2}} \int d\mathbf{r} \delta(\Phi(\mathbf{r}) - \phi) \delta(\Psi(\mathbf{r}) - \psi) e^{-\beta U_{\sigma_a\sigma_b}(\mathbf{r})} \right). \quad (72)$$

I. NUMERICAL PARAMETERS FOR FIGURES

Figures 2 - 5 use specific values for $H, H_{\text{enf}}, \mathbf{u}_a, \mathbf{u}_b, \mathbf{g}, \mathbf{h}$ and other parameters. For all figures, we use systems of 5 dimensions and choose diagonal Hessians so that the entries of \mathbf{u}_a and \mathbf{u}_b clearly describe the effect on the normal model. For all figures $\beta = 1$. The function diag takes a vector and returns a diagonal matrix with the vector's entries on the diagonal and $\text{normalize}(\mathbf{v}) = \mathbf{v}/\|\mathbf{v}\|$.

Parameters for Fig. 2

$$H = \text{diag}((10, 0.5, 10, 10, 10)), \mathbf{u}_a = \text{normalize}((0.0, 0.9, 0.1, 0, 0)), \mathbf{u}_b = \text{normalize}((0.9, 0.1, 0.0, 0.1, 0)).$$

Parameters for Fig. 3

$$H = \text{diag}((10, \lambda, 10, 10, 10)), \mathbf{u}_a = \text{normalize}((0.9, 0.1, 0.1, 0, 0)), \mathbf{u}_b = \text{normalize}((0.9, 0.1, 0.0, 0.1, 0)), \mathbf{g} = (g, 0, 0, 0, 0), f_a = f_b = 1, \mathbf{h} = -(f_a \mathbf{u}_a + f_b \mathbf{u}_b)/2.$$

Parameters for Fig. 4

$$H = \text{diag}((10, \lambda, 10, 10, 10)), H_{\text{dis}} = \text{diag}((0.01, 0.01, 0.01, 0.01, 0.01)), \mathbf{u}_a = \text{normalize}((0.0, 0.5, 0.5, 0, 0)), \mathbf{u}_b = \text{normalize}((0.0, 0.5, 0.0, 0.5, 0)), k_a = k_b = 1.$$

Parameters for Fig. 5 A

$$H = \text{diag}((1, 0.1, 1, 1, 1)), H_{\text{dis}} = \text{diag}((0.01, 0.01, 0.01, 0.01, 0.01)), \mathbf{u}_a = \text{normalize}((0.0, 0.5, 0.5, 0, 0)), \mathbf{u}_b = \text{normalize}((0.0, 0.5, 0.0, 0.5, 0)), f_a = f_b = 0.5, k_a = k_b = 0, \epsilon = 30, \mathbf{h} = -(f_a \mathbf{u}_a + f_b \mathbf{u}_b)/2, \mathbf{g} = (0, 0, 0, 0, 0).$$

Parameters for Fig. 5 B

$$H = \text{diag}((1, 1, 1, 1, 1)), H_{\text{dis}} = \text{diag}((0.01, 0.01, 0.01, 0.01, 0.01)), \mathbf{u}_a = \text{normalize}((0.5, 0.0, 0.5, 0, 0)), \mathbf{u}_b = \text{normalize}((0.5, 0.0, 0.0, 0.5, 0)), f_a = f_b = 0.5, k_a = k_b = 0, \epsilon = 30, \mathbf{h} = -(f_a \mathbf{u}_a + f_b \mathbf{u}_b)/2, \mathbf{g} = (5, 0, 0, 0, 0).$$

Parameters for Fig. 5 C

$$H = \text{diag}((1, 0.08, 1, 1, 1)), H_{\text{dis}} = \text{diag}((0.01, 0.01, 0.01, 0.01, 0.01)), \mathbf{u}_a = \text{normalize}((0.0, 0.5, 0.5, 0, 0)), \mathbf{u}_b = \text{normalize}((0.0, 0.5, 0.0, 0.5, 0)), f_a = f_b = 0, k_a = k_b = 0.5, \epsilon = 30, \mathbf{h} = (0, 0, 0, 0, 0), \mathbf{g} = (0, 0, 0, 0, 0).$$

Parameters for Fig. 5 D

$$H = \text{diag}((1, 1, 1, 1, 1)), H_{\text{dis}} = \text{diag}((0.01, 0.01, 0.01, 0.01, 0.01)), \mathbf{u}_a = \text{normalize}((0, 0, 1, 0, 0)), \mathbf{u}_b = \text{normalize}((0, 0, 0, 1, 0)), f_a = f_b = 0, k_a = k_b = 0.5, \epsilon = 12, \mathbf{h} = (0, 0, 0, 0, 0), \mathbf{g} = (0, 0, 0, 0, 0).$$

II. CONNECTION TO MWC MODEL

. Here we define an MWC model with two binding sites and show that the bistable and order-disorder cases reduce to the MWC model when there is no soft mode contribution to cooperativity.

MWC models make two assumptions : there exists an equilibrium of $k > 1$ states and, within each state, the binding free energies do not depend on whether a ligand is already bound (ie no cooperativity when locked in a single state). For simplicity, we assume the case of a symmetric protein so ligands bind to each site with the same binding energy for a given state. Denoting the free energy of the unbound condition of the k th state as $F_{00}^{(k)}$, the free energy of state k in the $i, j \in \{0, 1\}^2$ binding condition can be written as,

$$F_{ij}^{(k)} = F_{00}^{(k)} + (i + j)\Delta F^{(k)}. \quad (73)$$

The cooperativity, as before, is defined as $\Delta\Delta F = F_{10} + F_{01} - F_{00} - F_{11}$. The free energy of each ligand binding condition is calculated by summing over states, which in this case we consider $k = 2$, $F_{ij} = -\beta^{-1} \log \left(e^{-\beta F_{ij}^{(1)}} + e^{-\beta F_{ij}^{(2)}} \right)$. The cooperativity can be written as,

$$\Delta\Delta F = -\beta^{-1} \log \left[\frac{\left(e^{-\beta F_{10}^{(1)}} + e^{-\beta F_{10}^{(2)}} \right) \left(e^{-\beta F_{01}^{(1)}} + e^{-\beta F_{01}^{(2)}} \right)}{\left(e^{-\beta F_{00}^{(1)}} + e^{-\beta F_{00}^{(2)}} \right) \left(e^{-\beta F_{11}^{(1)}} + e^{-\beta F_{11}^{(2)}} \right)} \right] \quad (74)$$

Defining the difference in free energies of the apo states $\Delta F_{00} = F_{00}^{(2)} - F_{00}^{(1)}$ and the difference of binding energies $\Delta F = \Delta F^{(2)} - \Delta F^{(1)}$ gives the two MWC parameters. With these parameters the cooperativity becomes,

$$\Delta\Delta F = -\beta^{-1} \log \left[\frac{\left(e^{-\beta(F_{00}^{(1)} + \Delta F^{(1)})} + e^{-\beta(F_{00}^{(2)} + \Delta F^{(2)})} \right)^2}{\left(e^{-\beta F_{00}^{(1)}} + e^{-\beta F_{00}^{(2)}} \right) \left(e^{-\beta(F_{00}^{(1)} + 2\Delta F^{(1)})} + e^{-\beta(F_{00}^{(2)} + 2\Delta F^{(2)})} \right)} \right] \quad (75)$$

The free energies of state 2 can be written in terms of the free energies of state 1 and the differences,

$$\Delta\Delta F = -\beta^{-1} \log \left[\frac{\left(e^{-\beta(F_{00}^{(1)} + \Delta F^{(1)})} + e^{-\beta(F_{00}^{(1)} + \Delta F_{00} + \Delta F^{(1)} + \Delta F)} \right)^2}{\left(e^{-\beta F_{00}^{(1)}} + e^{-\beta(F_{00}^{(1)} + \Delta F_{00})} \right) \left(e^{-\beta(F_{00}^{(1)} + 2\Delta F^{(1)})} + e^{-\beta(F_{00}^{(1)} + \Delta F_{00} + 2\Delta F^{(1)} + 2\Delta F)} \right)} \right] \quad (76)$$

$$= -\beta^{-1} \log \left[\frac{\left(1 + e^{-\beta(\Delta F_{00} + \Delta F)} \right)^2}{\left(1 + e^{-\beta\Delta F_{00}} \right) \left(1 + e^{-\beta(\Delta F_{00} + 2\Delta F)} \right)} \right]. \quad (77)$$

The cooperativity is often in terms of equilibrium constants $c = e^{-\beta\Delta F}$ and $L = e^{-\beta\Delta F_{00}}$,

$$\Delta\Delta F = -\beta^{-1} \log \left[\frac{(1 + cL)^2}{(1 + L)(1 + c^2L)} \right] \quad (78)$$

Order-disorder Model : The order-disorder model ((18)) satisfies the two assumptions of the MWC model when $\mathbf{u}_a^\top H^+ \mathbf{u}_b = 0$. In this case, we can express ΔF and ΔF_{00} in terms of parameters of the order-disorder landscape (18). First we solve for ΔF_{00} . The free energy of the ordered and disordered apo states are,

$$F_{00}^{\text{ord}} = \frac{1}{2\beta} \log \left[\left(\frac{\beta h_0^2}{2\pi} \right)^{dN} \det H \right], \quad F_{00}^{\text{dis}} = \epsilon + \frac{1}{2\beta} \log \left[\left(\frac{\beta h_0^2}{2\pi} \right)^{dN} \det H_0 \right]. \quad (79)$$

Here det is the pseudo-determinant since H is singular. The difference between these is,

$$\Delta F_{00} = F_{00}^{\text{dis}} - F_{00}^{\text{ord}} = \epsilon + \frac{1}{2\beta} \log \left[\frac{\det H_0}{\det H} \right]. \quad (80)$$

Next, we solve for ΔF . The binding free energies in the ordered and disordered states are,

$$\Delta F^{\text{ord}} = \Delta F_{10}^{\text{ord}} - \Delta F_{00}^{\text{ord}} = \frac{1}{2\beta} \log \left[\left(\frac{\beta h_0^2}{2\pi} \right)^N \det H \right] - \frac{1}{2\beta} \log \left[\left(\frac{\beta h_0^2}{2\pi} \right)^N \det(H + k_a \mathbf{u}_a \mathbf{u}_a^\top) \right] = \frac{1}{2\beta} \log(1 + k_a \mathbf{u}_a^\top H^+ \mathbf{u}_a) \quad (81)$$

and,

$$\Delta F^{\text{dis}} = \Delta F_{10}^{\text{dis}} - \Delta F_{00}^{\text{dis}} = \frac{1}{2\beta} \log \left[\left(\frac{\beta h_0^2}{2\pi} \right)^N \det H_0 \right] - \frac{1}{2\beta} \log \left[\left(\frac{\beta h_0^2}{2\pi} \right)^N \det(H_0 + k_a \mathbf{u}_a \mathbf{u}_a^\top) \right] = \frac{1}{2\beta} \log(1 + k_a \mathbf{u}_a^\top H_0^+ \mathbf{u}_a). \quad (82)$$

Quantities from binding site b do not appear because of symmetry $\mathbf{u}_a^\top H^+ \mathbf{u}_a = \mathbf{u}_b^\top H^+ \mathbf{u}_b$ and $\mathbf{u}_a^\top H_0^+ \mathbf{u}_a = \mathbf{u}_b^\top H_0^+ \mathbf{u}_b$. Finally,

$$\Delta F = \Delta F^{\text{dis}} - \Delta F^{\text{ord}} = \frac{1}{2\beta} \log \left(\frac{1 + k_a \mathbf{u}_a^\top H_0^+ \mathbf{u}_a}{1 + k_a \mathbf{u}_a^\top H^+ \mathbf{u}_a} \right). \quad (83)$$

Bistable Model : The bistable model ((13)) satisfies the two assumptions of the MWC model when there are two minima : $\mathbf{g}^\top H^+ (\mathbf{h} + \mathbf{f} - \mathbf{g}) < 0 < \mathbf{g}^\top H^+ (\mathbf{h} + \mathbf{f} + \mathbf{g})$ and no cooperativity exists in each state $\mathbf{u}_a^\top H^+ \mathbf{u}_b = 0$. Here we express ΔF and ΔF_{00} in terms of parameters of the bistable landscape. Let state 1 be the basin in $\mathbf{g}^\top \mathbf{r} > 0$ and state 2 be the basin $\mathbf{g}^\top \mathbf{r} \leq 0$. We consider conditions where the basins are distinct (i.e. the barrier is larger than the temperature). First we solve for ΔF_{00} .

$$F_{00}^{(1)} = \frac{1}{2\beta} \log \left[\left(\frac{\beta h_0^2}{2\pi} \right)^N \det H \right] - \frac{1}{2} (\mathbf{h} + \mathbf{g})^\top H^+ (\mathbf{h} + \mathbf{g}), \quad F_{00}^{(2)} = \frac{1}{2\beta} \log \left[\left(\frac{\beta h_0^2}{2\pi} \right)^N \det H \right] - \frac{1}{2} (\mathbf{h} - \mathbf{g})^\top H^+ (\mathbf{h} - \mathbf{g}) \quad (84)$$

giving

$$\Delta F_{00} = F_{00}^{(2)} - F_{00}^{(1)} = 2\mathbf{h}^\top H^+ \mathbf{g} \quad (85)$$

Now we solve for ΔF_{00} . Since the ligand binding applies a force, the curvature does not change, and the binding free energies only depend on the change in the energy minimum. Because we assume a symmetric protein, we can write the free energies in terms of either binding site. Here we choose site a .

$$\Delta F^{(1)} = F_{10}^{(1)} - F_{00}^{(1)} = -\frac{1}{2} f_a^2 \mathbf{u}_a^\top H^+ \mathbf{u}_a - f_a \mathbf{u}_a^\top H^+ \mathbf{h} - f_a \mathbf{u}_a^\top H^+ \mathbf{g} \quad (86)$$

and instead

$$\Delta F^{(2)} = F_{10}^{(2)} - F_{00}^{(2)} = -\frac{1}{2} f_a^2 \mathbf{u}_a^\top H^+ \mathbf{u}_a - f_a \mathbf{u}_a^\top H^+ \mathbf{h} + f_a \mathbf{u}_a^\top H^+ \mathbf{g}. \quad (87)$$

Finally,

$$\Delta F = \Delta F^{(2)} - \Delta F^{(1)} = 2f_a \mathbf{u}_a^\top H^+ \mathbf{g}. \quad (88)$$

TWO PHYSICAL PRINCIPLES ENABLE ALLOSTERY : ARBITRARY V_a, V_b

In the main text, we considered ligand potentials that act along one mode of the binding site. $V_a(\mathbf{r}_a) = g_a(\mathbf{u}_a^\top \mathbf{r})$, $V_b(\mathbf{r}_b) = g_b(\mathbf{u}_b^\top \mathbf{r})$. Here we relax this assumption and find the same results.

We partition the degrees of freedom of the system, into degrees of freedom that describe binding site a , \mathbf{r}_a , binding site b , \mathbf{r}_b , and the rest of the degrees of freedom, \mathbf{r}_r such that $\mathbf{r} = (\mathbf{r}_a, \mathbf{r}_r, \mathbf{r}_b)$. With this notation, we can write the four energy landscapes with ligand potentials as a function of either \mathbf{r}_a or \mathbf{r}_b . we can write the four ligation conditions,

$$U_{\sigma_a \sigma_b}(\mathbf{r}) = U_p(\mathbf{r}) + \sigma_a V_a(\mathbf{r}_a) + \sigma_b V_b(\mathbf{r}_b) \quad (89)$$

and the partition functions as,

$$Z_{\sigma_a \sigma_b} = \int d\mathbf{r} d\mathbf{x}_a d\mathbf{x}_b \delta(\mathbf{r}_a - \mathbf{x}_a) \delta(\mathbf{r}_b - \mathbf{x}_b) e^{-\beta U_p(\mathbf{r}) - \sigma_a \beta V(\mathbf{x}_a) - \sigma_b \beta V(\mathbf{x}_b)} \quad (90)$$

$$= \int d\mathbf{x}_a e^{-\sigma_a \beta V(\mathbf{x}_a)} \int d\mathbf{x}_b e^{-\sigma_b \beta V(\mathbf{x}_b)} \int d\mathbf{r} \delta(\mathbf{r}_a - \mathbf{x}_a) \delta(\mathbf{r}_b - \mathbf{x}_b) e^{-\beta U_p(\mathbf{r})} \quad (91)$$

$$= \int d\mathbf{x}_a e^{-\sigma_a \beta V(\mathbf{x}_a)} \int d\mathbf{x}_b e^{-\sigma_b \beta V(\mathbf{x}_b)} \tilde{Z}(\mathbf{x}_a, \mathbf{x}_b) \quad (92)$$

with $\tilde{Z}(\mathbf{x}_a, \mathbf{x}_b) = \int d\mathbf{r} \delta(\mathbf{r}_a - \mathbf{x}_a) \delta(\mathbf{r}_b - \mathbf{x}_b) e^{-\beta U_p(\mathbf{r})}$. As before we have chosen units where the length scale h_0 of the partition function is one and is omitted. Using the Fourier transform definition of the multivariate delta function,

$$\delta(\mathbf{t}) = \int_{-\infty}^{\infty} d\mathbf{s} e^{-2\pi i \mathbf{s}^\top \mathbf{t}}, \quad (93)$$

we get,

$$\tilde{Z}(\mathbf{x}_a, \mathbf{x}_b) = \int d\mathbf{r} \int d\mathbf{s}_a e^{-2\pi i \mathbf{s}_a^\top (\mathbf{r}_a - \mathbf{x}_a)} \int d\mathbf{s}_b e^{-2\pi i \mathbf{s}_b^\top (\mathbf{r}_b - \mathbf{x}_b)} e^{-\beta U_p(\mathbf{r})} \quad (94)$$

$$= \int d\mathbf{s}_a e^{2\pi i \mathbf{s}_a^\top \mathbf{x}_a} \int d\mathbf{s}_b e^{2\pi i \mathbf{s}_b^\top \mathbf{x}_b} \int d\mathbf{r} e^{-\beta U_p(\mathbf{r}) - 2\pi i \mathbf{s}_a^\top \mathbf{r}_a - 2\pi i \mathbf{s}_b^\top \mathbf{r}_b}. \quad (95)$$

Now we use F_p of (7) to approximate any U_p . and define the vector $\mathbf{s} = (\mathbf{s}_a, \mathbf{0}, \mathbf{s}_b)$.

$$\tilde{Z} = \sum_{i=1}^n \int d\mathbf{s}_a e^{2\pi i \mathbf{s}_a^\top \mathbf{x}_a} \int d\mathbf{s}_b e^{2\pi i \mathbf{s}_b^\top \mathbf{x}_b} \int d\mathbf{r} e^{-\beta (\frac{1}{2}(\mathbf{r} - \mathbf{R}_i)^\top H_i (\mathbf{r} - \mathbf{R}_i) + \epsilon_i) - 2\pi i \mathbf{s}^\top \mathbf{r}} \quad (96)$$

$$= \sum_{i=1}^n e^{-\beta \epsilon_i} \int d\bar{\mathbf{s}} e^{2\pi i \bar{\mathbf{s}}^\top \bar{\mathbf{x}}} \int d\mathbf{y}_i e^{-\beta \frac{1}{2} \mathbf{y}_i^\top H_i \mathbf{y}_i - 2\pi i \bar{\mathbf{s}}^\top (\mathbf{y}_i + \mathbf{R}_i)} \quad (97)$$

$$= \sum_{i=1}^n e^{-\beta \epsilon_i} \int d\bar{\mathbf{s}} e^{2\pi i \bar{\mathbf{s}}^\top (\bar{\mathbf{x}} - \bar{\mathbf{R}}_i)} \int d\mathbf{y}_i e^{-\beta \frac{1}{2} \mathbf{y}_i^\top H_i \mathbf{y}_i - 2\pi i \bar{\mathbf{s}}^\top \mathbf{y}_i} \quad (98)$$

$$= \sum_{i=1}^n e^{-\beta \epsilon_i} \sqrt{\frac{(2\pi)^{dN}}{\beta \det(H_i)}} \int d\bar{\mathbf{s}} e^{2\pi i \bar{\mathbf{s}}^\top (\bar{\mathbf{x}} - \bar{\mathbf{R}}_i)} e^{-2\pi^2 \beta^{-1} \bar{\mathbf{s}}^\top H_i^+ \bar{\mathbf{s}}} \quad (99)$$

$$= \sum_{i=1}^n e^{-\beta \epsilon_i} \sqrt{\frac{(2\pi)^{dN}}{\beta \det(H_i)}} \int d\bar{\mathbf{s}} e^{2\pi i \bar{\mathbf{s}}^\top (\bar{\mathbf{x}} - \bar{\mathbf{R}}_i)} e^{-2\pi^2 \beta^{-1} \bar{\mathbf{s}}^\top \bar{G}_i \bar{\mathbf{s}}} \quad (100)$$

$$= \sum_{i=1}^n e^{-\beta \epsilon_i} \sqrt{\frac{(2\pi)^{dN}}{\beta \det(H_i)}} \int d\bar{\mathbf{s}} e^{-2\pi^2 \beta^{-1} \bar{\mathbf{s}}^\top \bar{G}_i \bar{\mathbf{s}} + 2\pi i (\bar{\mathbf{x}} - \bar{\mathbf{R}}_i)^\top \bar{\mathbf{s}}} \quad (101)$$

$$= \sum_{i=1}^n \sqrt{\frac{(2\pi)^{dN}}{\beta \det(H_i)}} \sqrt{\frac{(2\pi)^l}{\det(4\pi^2 \beta^{-1} \bar{G}_i)}} e^{-\frac{1}{2} \beta (\bar{\mathbf{x}} - \bar{\mathbf{R}}_i)^\top \bar{G}_i^{-1} (\bar{\mathbf{x}} - \bar{\mathbf{R}}_i) - \beta \epsilon_i} \quad (102)$$

$$(103)$$

On the second line we introduced $\mathbf{y}_i = \mathbf{r} - \mathbf{R}_i$, $\bar{\mathbf{s}} = (\mathbf{s}_a, \mathbf{s}_b)$ and $\bar{\mathbf{x}} = (\mathbf{x}_a, \mathbf{x}_b)$. On the third line we introduce $\bar{\mathbf{R}}_i = (\mathbf{R}_i^a, \mathbf{R}_i^b)$ where $\mathbf{R}_i = (\mathbf{R}_i^a, \mathbf{R}_i^r, \mathbf{R}_i^b)$ describes the same way of partitioning the vector's entries into those

associated with binding site a , binding site b and the rest, as was done for $\mathbf{r} = (\mathbf{r}_a, \mathbf{r}_r, \mathbf{r}_b)$. On the fifth line we introduced $\bar{G}_i = \begin{pmatrix} H_{i,aa}^+ & (H_{i,ab}^+)^\top \\ H_{i,ab}^+ & H_{i,bb}^+ \end{pmatrix}$ where $H_{i,aa}^+, H_{i,ab}^+, H_{i,bb}^+$ are sub matrices of H_i^+ that contain the entries that contribute to the product $\mathbf{s}^\top H_i^+ \mathbf{s}$. On the last line, l is the number of dimensions of $\bar{\mathbf{s}}$. The resulting free energy surface is,

$$\tilde{F}(\mathbf{x}_a, \mathbf{x}_b) = -\frac{1}{\beta} \log \left(\sum_{i=1}^n \sqrt{\frac{(2\pi)^{dN}}{\beta \det(H_i)}} \sqrt{\frac{(2\pi)^l}{4\pi^2 \beta^{-1} \det(\bar{G}_i)}} e^{-\frac{1}{2}\beta(\bar{\mathbf{x}} - \bar{\mathbf{R}}_i)^\top \bar{G}_i^{-1}(\bar{\mathbf{x}} - \bar{\mathbf{R}}_i) - \beta\epsilon_i} \right). \quad (104)$$

When there is one state $n = 1$ (we drop the subscript), the free energy surface, up to a constant, is

$$\tilde{F}(\mathbf{x}_a, \mathbf{x}_b) = \frac{1}{2}(\bar{\mathbf{x}} - \bar{\mathbf{R}})^\top \bar{G}^{-1}(\bar{\mathbf{x}} - \bar{\mathbf{R}}). \quad (105)$$

G is a 2 by 2 block matrix. The inverse of a symmetric 2 by 2 block matrix is,

$$\begin{pmatrix} A & B^\top \\ B & C \end{pmatrix}^{-1} = \begin{pmatrix} A^{-1} + A^{-1}B^\top(C - BA^{-1}B^\top)^{-1}BA^{-1} & -A^{-1}B^\top(C - BA^{-1}B^\top)^{-1} \\ -(C - BA^{-1}B^\top)^{-1}BA^{-1} & (C - BA^{-1}B^\top)^{-1} \end{pmatrix} \quad (106)$$

The free energy surface is separable when the off-diagonal block of G^{-1} is zero. That is when

$$(H_{bb}^+ - H_{ab}^+(H_{aa}^+)^{-1}(H_{ab}^+)^\top) H_{ab}^+(H_{aa}^+)^{-1} = 0 \quad (107)$$

If we assume that H_{aa}^+ and H_{bb}^+ are invertible, non-zero, and have finite entries, then the solution occurs when $H_{ab}^+ = 0$, that is there is no correlation between the degrees of freedom at binding site a and binding site b .